TTCCAG-3′ and 5′-TTCAGTCCAAGCATACTGGTCCTTTC-CAAG-3′.

The tool for sequence homology search was BLAST [31], whereas that for multiple sequence alignment was CLUSTALW.

Construction of cDNA expression vectors

cDNA sequences of marmoset genes used in this study were based on AF452616 as *CD4*, DQ189217 as *CD8a*, DQ520834 as *CD25*, AB097501 as *CD34*, and AB097502 as *CD117*. RNA was extracted from cells by Isogen (Nippon Gene Co. Ltd., Tokyo, Japan) and reverse-transcribed to cDNA by Superscript (Invitrogen, Carlsbad, CA, USA). A portion of cDNA sequence corresponding to an extracellular domain of the protein was amplified by a PCR method, using cDNA as a template and AccuPrime Pfx DNA Polymerase (Invitrogen, Tokyo, Japan). The set of forward and reverse primers used were as follows: for *IL-2*, 5′-ATGTACAG-CATGCAGCTCGC-3′ and 5′-GCTTTGACAGAAGGCTATCC-3′; for *CD4*, 5′-CCACCATGAATGGGGGAATCCCTTTC-3′ and 5′-CACCGGGGGAGACCATGTGGGCA-3′; for *CD8α*, 5′-CCAC CATGGCCTCGCCAGTGACCGC-3′ and 5′-ACAGGCGAAGT CCAGCCCC-3′; for *CD25*, 5′-CCACCATGGATTCACAACTG CTGATG-3′ and 5′-CTTCGTCGTAAGTATGAATGTCTCC-3′; for *CD34*, 5′-ATGCTGGTCCGCAGGGGC-3′ and 5′-TCGGGAA TAACTCTGGTGGCTTGC-3′; for *CD45*, 5′-CCACCATG-TATTTGTGGCTTAAACTGCT-3′ and 5′-TGATTGAAATTTAC-TAACTGGGTG-3′; for *CD117*, 5′-CCACCATGAGA GGCGCTCGTGGCG-3′ and 5′-GAACAGGGTGTGGGGCTG-GATTTGC-3′. Each PCR product was inserted into the *EcoR*V site of pCXGFP-1 vector (GenBank, Accession No. AB281497) in order to express an extracellular domain of interest as a fusion protein with an enhanced EGFP.

Preparation of cDNA-transfected cells

pCXGFP-1 vectors expressing marmoset cDNAs were transfected into Chinese hamster ovary (CHO) cells by electroporation using Gene Pulser (BioRad, Tokyo, Japan) according to manufacturer's instructions. After G418 selection at 1 mg/mL, the GFP^+ cells were isolated by fluorescence-activated cell sorter.

Production of mAbs

We adopted the hydrodynamic immunization procedure reported by Song et al. [32]. Briefly, 25 mg pCX-GFP plasmid DNA was suspended in 2 mL saline and injected intravenously into BALB/c mice. Mice were immunized three to six times, and serum antibody titers were checked by flow cytometric analyses using cDNA-transfected cells as a source of antigen. Four days after a final boost, mice were sacrificed and splenocytes were fused with the mouse myeloma cell line P3U1 according to a standard procedure. Positive clones were identified by flow cytometry, isolated, expanded, and stocked.

Preparation of human blood cells

Human umbilical cord blood was obtained from full-term healthy newborns immediately after vaginal delivery. Informed consent was obtained from individual mothers according to the institutional guidelines, and the work was approved by the Tokai University Human Research Committee. Peripheral blood was collected from healthy human volunteers. Mononuclear cells were isolated from cord and peripheral blood by Ficoll-Paque (GE Healthcare Biosciences, Uppsala, Sweden) gradient centrifugation as reported previously [15].

Preparation and stimulation of marmoset lymphocytes

Thymi, intestinal lymph modes, or spleens were taken from marmosets and cells were released from the tissues. After red blood cells were lysed osmotically, cells were suspended in RPMI-1640 medium containing 10% fetal calf serum. Peripheral blood or bone marrow cells were collected from marmosets with heparin and centrifuged on Lymphocepal (IBL Co., Takasaki, Japan) at 2,000 rpm for 30 minutes. Mononuclear cells were collected and the remaining erythrocytes were lysed.

To stimulate T cells, the cells were cultured in medium supplemented with anti-human CD3 (SP34-2; BD Pharmingen, San Diego, CA, USA) and anti-human CD28 (CD28.2; eBioscience, San Diego, CA, USA) or TSST-1 (1 mg/mL; Toxin Tec. Co., Sarasota, FL, USA) for 24 hours. Then, the cells were harvested, incubated with anti-marmoset CD4 or CD8 mAb (prepared in this study) or anti-human CD20 mAb (B-Ly1, Dako, Glostrup, Denmark) at 4°C for 15 minutes, washed, and reincubated with anti-mouse IgG–magnetic cell sorting (MACS) micro beads for 15 minutes. After a final wash, CD4-, CD8- or CD20-positive cells were purified using a MACS system (Miltenyi Biotec, Gladbach, Germany).

Colony-forming assay using bone marrow–derived mononuclear cells

Cells were recovered from bone marrow of the common marmoset, and a mononuclear fraction was isolated using Lymphoprep (Axis-Shield, Oslo, Norway). Then cells were sorted into $CD34^+CD117^+$, $CD34^+CD117^-$, $CD34^-CD117^+$, and $CD34^-CD117^-$ fractions using FACS Aria (Becton Dickinson, Franklin Lakes, NJ, USA). Anti-marmoset CD34 mAb was reported previously [29], and anti-marmoset CD117 mAb was prepared in the present study. The sorted cells in each group were plated at 2×10^2 cells in 1 mL methylcellulose-containing medium (Methocult GF+ H4435; Stem Cell Technologies, Vancouver, Canada) in a 35-mm dish with human stem cell factor (SCF) (10 ng/mL), IL-3 (10 ng/mL), human erythropoietin (Epo) (2 U/mL), and human G-CSF (10 ng/mL) and cultured at 37°C in a 5% CO_2 atmosphere. After 14 days of culture, types and numbers of hematopoietic colonies (colony-forming units [CFU]) were counted according to standard criteria. Samples from one animal were processed for the assay in triplicate, and two different animals were used (experiments 1 and 2).

Transplantation of hematopoietic progenitors into NOG mice

$CD34^+CD117^+$ and $CD34^-CD117^+$ cells were purified from bone marrow of the common marmoset by cell sorter as described here. Purity was >98% according to flow cytometry. Nine-week-old NOG mice were irradiated with 2.5 Gy x-ray prior to transplantation, and the marmoset cells (6.7×10^5 for $CD34^+CD117^+$ cells/ 1.3×10^6 for $CD34^-CD117^+$ cells) were transplanted intravenously. Four weeks after transplantation, peripheral blood was collected via orbit under inhalation anesthesia. Mononuclear cells were prepared and reconstitution efficiency was calculated by the ratio of marmoset $CD45^+$ cells.

Flow cytometric analysis

Cells were incubated with labeled primary mAb for 15 minutes at 4°C and washed with 1% (w/v) bovine serum albumin-containing phosphate-buffered saline. In some cases, cells were reincubated with labeled secondary antibody. The flow cytometer was FACSCalibur

(Becton Dickinson). The mAbs used were as follows: purchased from BD Pharmingen were anti-human CD3-peridinin chlorophyll Cy5.5 (PerCP) (SP34-2), anti-human CD4-allophycocyanin (APC) (SK3), anti-human CD8–fluorescein isothiocyanate (FITC) (HIT8a), anti-human CD20 (B-Ly1), anti-human CD25-phycoerythrin (PE) (M-A251), anti-human CD34 (581), anti-human CD45-APC (HI30), anti-human CD117-APC (YB5.B8), streptavidine-PE and streptavidine-APC. Purchased from eBioscience were anti-mouse CD4-APC (GK1.5), anti-mouse CD8-FITC (53.67), anti-mouse CD45.1-APC (30-F11), anti-mouse CD25-PE (PC61) and anti-mouse CD34 (RAM34). Anti-mouse CD117-APC (3C1) was from CALTAG Laboratories (Burlingame, CA, USA), and anti-mouse IgM-PE and anti-mouse IgG-PE were from Jackson ImmunoResearch Inc. (West Grove, PA, USA). We previously obtained anti-marmoset CD8 and CD45 mAbs by a different approach from that taken in this study [33]. These two mAbs were used as controls in the present study.

Results

cDNA expression systems and generation of mAbs

In the previous study, we cloned and sequenced 37 cDNA of immune-related genes obtained from marmoset spleen cells. Among them, we selected CD4, CD8, CD25, CD45, and CD117 as the targets to develop mAbs against marmoset proteins in this study. In humans and mice, CD4, CD8, and CD25 are representative surface molecules of T lymphocytes, CD117, and CD34 are hallmarks of hematopoietic progenitors, and CD45 represents a pan-leukocyte antigen.

To express a marmoset-derived cDNA, a pCXGFP1 vector was used (Fig. 1A). A cDNA portion encoding an extracellular domain of marmoset protein of interest to us was inserted into the *EcoR*V cloning site. From a recombinant, a marmoset cDNA was expressed as a fusion protein with the transmembrane domain of human MICA and cytoplasmically located enhanced GFP. Transcription was driven by CAG promoter. This recombinant was injected into mice as a DNA vaccine to sensitize the animals. In parallel, for the purpose of screening antibody production, a source of antigen was prepared by transfecting this expression plasmid into CHO cells. The cells expressing a fusion protein were selected by incubating the culture in the presence of G418. The plasmid harbored the neomycin-resistant gene.

By conventional experimental procedures, we could isolate the following six mAb clones (a subclass of Ig indicated). They were the clone Mar4-33 producing anti-CD4 mAb (IgG1), the clone Mar8-10 producing anti-CD8 mAb (IgG1), the clone Mar25-3 producing anti-CD25 mAb (IgG1), the clone Mar45-14 producing anti-CD45 mAb (IgG1), the clone MA24 producing anti-CD34 mAb (IgM), and the clone Mar117-22 producing anti-CD117 mAb (IgG1). Each mAb, including the previously described clone MA24, that produces anti-CD34 IgM mAb [29] was labeled with fluorochrome.

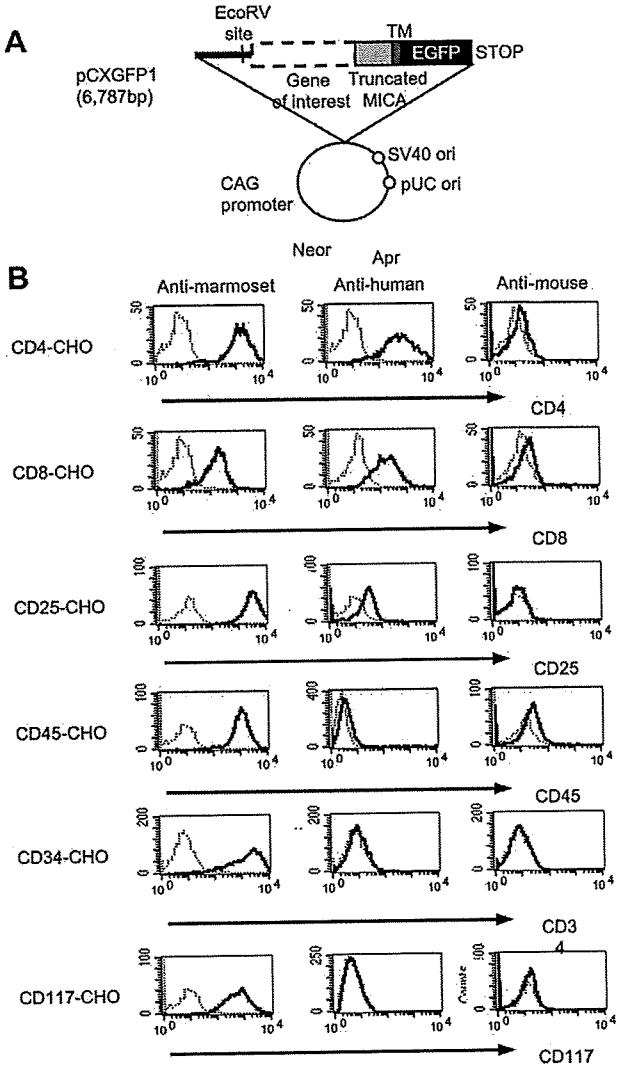

Figure 1. Reactivity of anti-marmoset, anti-human, and anti-mouse monoclonal antibodies (mAbs) against marmoset proteins expressed on CHO cells. (**A**) Schematic illustration of cDNA-expressing pCXGFP-1 vector. The *EcoR*V site is a cloning site of cDNA whose expression is driven by a CAG promoter. A gene of interest is expressed as a fusion protein with a transmembrane (TM) domain of human MICA and an intracytoplasmically located enhanced green fluorescent protein (EGFP) protein. The neomycin-resistance gene (Neor) is a drug selection marker. (**B**) Flow cytometric analyses of marmoset cDNA-expressing CHO cells stained by anti-marmoset, anti-human and anti-mouse mAbs.

Characterization of anti-marmoset mAbs

Figure 1B illustrates flow cytometric profiles of marmoset cDNA-transfected CHO cells stained by the newly prepared 6 mAbs and commercial mAbs. As can be seen in the left columns, each of the generated anti-marmoset mAb reacted with the respective antigen on CHO cells to a substantial degree of fluorescence intensity. This confirmed the authenticity of each mAb to recognize the respective antigen.

Cross-reactivity of anti-human mAb was examined in parallel (middle columns) using the cDNA-transfected CHO cells. An anti-human CD4 mAb (SK3) cross-reacted with marmoset CD4 as efficiently as anti-marmoset CD4 mAb. An anti-human CD8 mAb (HIT8α) gave a similar result. On the other hand, an anti-human CD25 mAb (M-A251) weakly cross-reacted with marmoset CD25, whereas anti-human CD45 (HI30), anti-human CD34 (581), and anti-human CD117 (YB5.B8) mAbs did not cross-react at all with the corresponding marmoset antigens. None of the anti-mouse mAbs showed any cross-reactivity with marmoset antigens (right columns).

Detection of marmoset T lymphocytes by anti-marmoset CD4 and CD8 mAbs

As shown in Figure 1B, the anti-marmoset mAbs reacted with the marmoset antigen that was overexpressed from transfected cDNA. Then, we investigated the reactivity of the same mAbs toward endogenously expressed marmoset antigens. As for the cells endogenously expressing these antigens, marmoset spleen cells were examined for reactivity of mAbs against marmoset CD4 and CD8 by two-color flow cytometric analysis. In the left panel of Figure 2A, marmoset splenocytes were stained by anti-marmoset CD4 and anti-human CD4 mAbs. The existence of double-positive cells in the upper right quadrant indicates the recognition of the same molecule by the two antibodies. A similar result was obtained when anti-marmoset CD8 and anti-human CD8 mAbs were used (see right panel of Fig. 2A).

CD3 is a pan-T lineage marker. We confirmed that an anti-human CD3ε mAb (SP34-2) recognized marmoset CD3ε-transfected cells (data not shown). In fact, marmoset splenocytes were stained with anti-human CD3ε and anti-marmoset CD4, or anti-human CD3ε and anti-marmoset CD8 mAbs, respectively (Fig. 2B). The $CD3\varepsilon^+$ T lymphocytes were divided into $CD4^+$ and $CD8^+$ cells. The combination of anti-human CD3ε and anti-human CD4 mAbs, or that of anti-human CD3ε and anti-human CD8 mAbs, gave the same result. It must be noted that anti-marmoset CD4 and anti-marmoset CD8 mAbs did not react with human peripheral blood mononuclear cells (Fig. 2C), indicating that anti-marmoset mAbs do not recognize the corresponding human antigens.

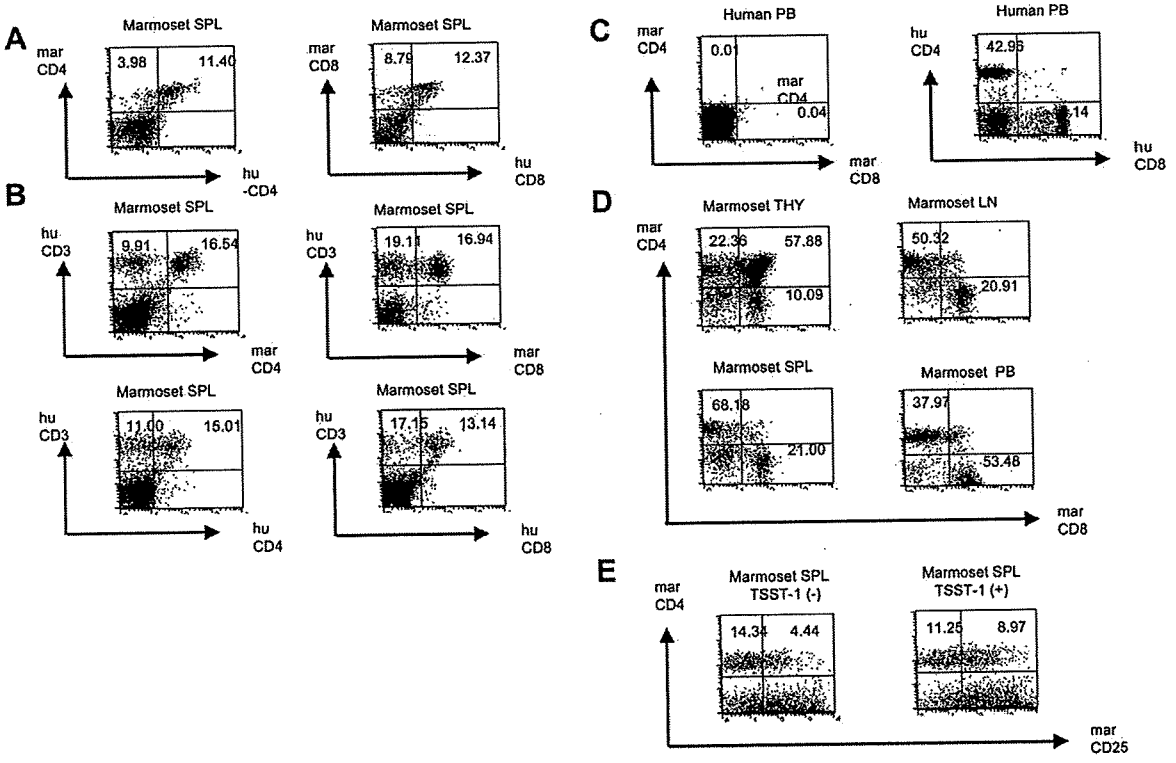

Figure 2. Characterization of anti-marmoset CD4, CD8, and CD25 monoclonal antibodies (mAbs), and identification of marmoset $CD4^+$ and $CD8^+$ T lymphocytes. (**A**, **B**) Marmoset splenocytes (SPL) were stained by the indicated mAbs, and their flow cytometric patterns are displayed. The mAbs used were anti-marmoset CD4, anti-marmoset CD8, anti-human CD4, anti-human CD8 and anti-human CD3ε. (**C**) Flow cytometry of human peripheral blood (PB) mononuclear cells. The mAbs were used as indicated. (**D**) Flow cytometry of marmoset-derived thymocytes (THY), SPL, lymph node cells (LN), and PB mononuclear cells. Anti-marmoset CD4 and CD8 mAbs were used as indicated. (**E**) Flow cytometry of marmoset SPL stained with anti-marmoset CD4 and anti-marmoset CD25 mAbs. Freshly isolated splenocytes (left) and the cells treated with TSST-1 in vitro (right) were analyzed.

Table 1. Comparison of Callithrix jacchus–derived CD34 and c-kit with human and mouse orthologs

Protein	Identical aa residues (%)		
	Marmoset vs human	Marmoset vs mouse	Human vs mouse
CD34	80	60	63
c-kit	94	81	82

Amino acid sequences of CD34 and c-kit from common marmoset (BAD04017.1 and BAD04018.1, respectively) were compared by BLAST homology search with human and mouse orthologs (human CD34, NP_001020280.1; human c-kit, NP_000213.1; mouse CD34, NP_598415.1; mouse c-kit, NP_066922.1) in three way pair-wise comparisons. The numbers indicate the percentages of identical aa residues between the two proteins compared.

These results confirmed that anti-marmoset CD4 and CD8 mAbs indeed recognize endogenous molecules. Then we also examined the distribution of T-cell subsets in other marmoset lymphoid tissues using these two mAbs (Fig. 2D). In marmoset thymi, the four subpopulations detected were $CD4^-CD8^-$, $CD4^+CD8^+$, $CD4^+CD8^-$, and $CD4^-CD8^+$, whereas only the two mature subsets $CD4^+CD8^-$ and $CD4^-CD8^+$ were detected in marmoset peripheral lymphoid tissues, such as spleen, lymph node, and peripheral blood. The profiles of these T-cell subsets were indistinguishable from those seen in human and mouse lymphoid tissues.

CD25 has been identified as an activation marker expressed on T cells in mice and humans. Then, mAb against marmoset CD25 was used to determine whether CD25 is expressed on marmoset splenocytes pre- and/or poststimulated with TSST-1 superantigen derived from *Staphylococcus aureus*, which can strongly stimulate $CD4^+$ T cells via T cell receptor (TCR)-β chain. The results showed an increase of CD25-expressing cells in $CD4^+$ cells (23–44%) after TSST-1 stimulation, indicating that CD25 is induced to express via T-cell activation in marmosets as well as in humans. A relative proportion of $CD25^+$ cells without CD4 expression in both pre– and post–TSST-1 stimulation was observed (Fig. 2E), and these $CD4^-CD25^+$ cells may belong to non–T cells, such as B cells and dendritic cells (DCs), as will be discussed later.

Cytokine gene expression profiles in marmoset T lymphocytes

Because the existence of $CD4^+$ and $CD8^+$ fractions was confirmed in lymphoid tissues, we then examined the cytokine expression profiles in marmoset T lymphocytes. To purify $CD4^+$ and $CD8^+$ cells from marmoset spleens, biotin-labeled anti-marmoset mAbs were used. As a control, B lymphocytes were isolated using anti-human CD20 mAb, because a transfectant expressing marmoset CD20 was recognized by anti-human CD20 (data not shown). The spleen cells were stimulated in vitro by anti-human CD3ε mAb, anti-human CD3ε, and anti-human CD28 mAbs, or superantigen TSST-1. After that, CD4 T cells were purified and RNA was prepared from the cells for semi-quantitative RT-PCR analyses (Fig. 3). Primers were designed based on published sequences of marmoset cDNAs.

In splenic $CD4^+$ cells (Fig. 3A), transcripts of *IL-4, IL-5, IL-6, IL-10, IL-17A, IL-17F,* and *IFN-γ* were barely or only slightly detected prior to stimulation, but were induced substantially by T-cell stimulation. *IL-2* induction was observed only after stimulation by TSST-1. In contrast, a relatively high amount of transcripts was detected for *TGF-β* and *TNF-α* prior to stimulation, and their expression persisted after stimulation. All of the $CD4^+$cells freshly isolated from five marmosets' peripheral blood showed a similar transcription profile to those in spleen cells (Fig. 3B).

$CD8^+$ splenic T cells were also examined (Fig. 3C). *IL-2* transcript was not detected before stimulation, but was substantially induced by TCR-mediated stimulations. Expression of *granzyme B* and *IFN-γ* was moderately

Table 2. Colony formation of marmoset bone marrow progenitor cells

Group[a]	CFU-mix[b]	CFU-G[b]	CFU-GM[b]	CFU-M[b]	Mega[b]	GFU-E/CFU-E[b]
Experiment 1						
$CD34^+/c\text{-}kit^+$	2 ± 1.4	6.3 ± 1.7	5.3 ± 1.9	0.3 ± 0.5	1 ± 1.4	2 ± 0.8
$CD34^+/c\text{-}kit^-$	0 ± 0	1.3 ± 0.5	0.7 ± 0.9	2 ± 0	1 ± 0	1 ± 0.8
$CD34^-/c\text{-}kit^+$	1.3 ± 0.5	5.3 ± 1.2	3.0 ± 0.8	0.3 ± 0.5	0 ± 0	4.0 ± 1.6
$CD34^-/c\text{-}kit^-$	0.7 ± 0.9	2 ± 0.8	1 ± 0.8	0 ± 0	1 ± 0	0.7 ± 0.9
Experiment 2						
$CD34^+/c\text{-}kit^+$	4.3 ± 2.1	12 ± 2.9	12 ± 1.6	1.7 ± 0.5	0.3 ± 5	6 ± 0.8
$CD34^+/c\text{-}kit^-$	0 ± 0	0.3 ± 0.5	0 ± 0	2 ± 0	0 ± 0	0 ± 0
$CD34^-/c\text{-}kit^+$	1.0 ± 0.8	8.7 ± 1.7	9.0 ± 3.7	5.0 ± 0	0.3 ± 0.5	6.7 ± 1.9
$CD34^-/c\text{-}kit^-$	0 ± 0	0.3 ± 0.5	0.7 ± 0.5	4 ± 1.4	0 ± 0	0 ± 0

Data are expressed as mean ± standard deviation.

[a]Marmoset bone marrow cells were sorted to four fractions according to CD34 and c-kit expressions and cultured in methylcellulose-containing medium for 2 weeks.

[b]Colony-forming unit (CFU)-mix, colony-forming unit granulocyte (CFU-G), colony-forming unit granulocyte-macrophage (CFU-GM), colony-forming unit macrophage (CFU-M), megakaryocyte (Mega)/colony-forming unit erythroid (GFU/CFU-E)/2 × 10^2 sorted bone marrow cells are shown. Colonies in triplicate were counted by microscopy. One marmoset per experiment was used.

detected before stimulation, and was significantly upregulated by stimulation. In contrast, *perforin-1* expression was sufficiently detected without stimulation and did not show any enhancement with stimulation.

Overall, the expression profiles of various cytokine genes seen in marmoset T cells were generally similar to those observed in humans and mice.

A primary structure of marmoset granzyme B gene

In the previously described plasmid construction and RT-PCR analyses, we utilized marmoset cDNA sequences that had mostly been reported in our previous study [28]. Exceptions were *perforin 1* and *granzyme B*. The nucleotide and deduced amino acid sequences of these two genes were newly determined in this study and were registered at National Center for Biotechnology Information (NCBI) as EU918127 and EU918128, respectively.

An interesting feature was observed in the primary sequence of *granzyme B* transcript (Fig. 4). Near the carboxy terminus of open reading flame, an additional sequence of 317 nt was inserted, which was not found in the corresponding region of human and chimpanzee *granzyme B* (see the sequence indicated by blue in (Fig. 4A), and note that Hs, Pt, and Cj represent human, chimpanzee and the common marmoset, respectively). This insertion caused a shift in the reading frame (see the location of termination codon indicated by red). Thus, the number of amino acid residues in the predicted marmoset polypeptide became longer by 23 aa at its carboxy terminus compared to human and chimpanzee granzyme B proteins (Fig. 4B). We cloned the genomic DNA from marmoset peripheral blood cells, and confirmed the insertion of the sequence in question into the exactly corresponding site of *granzyme B* gene (data not shown). Interestingly, the BLAST tool revealed a close homology of the inserted sequence to the

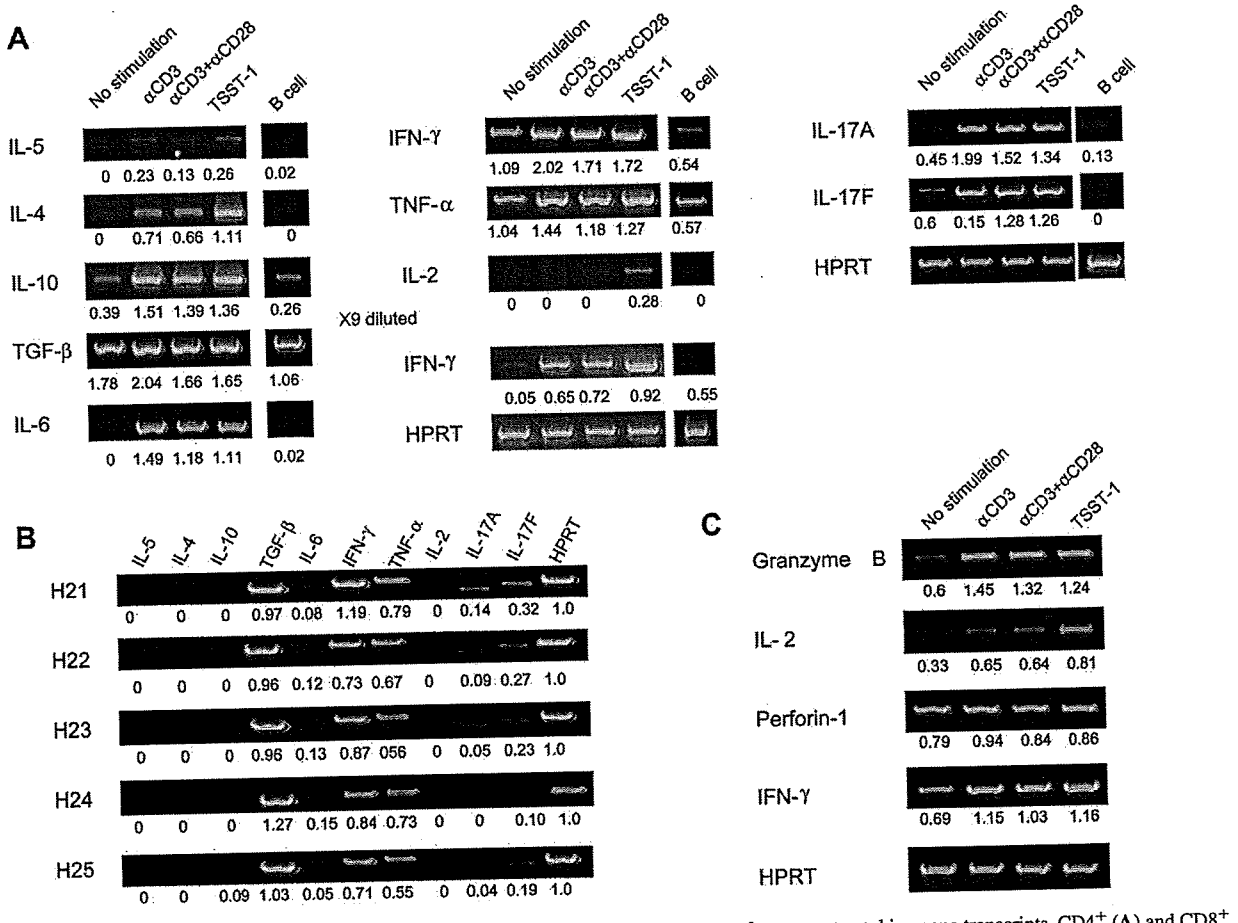

Figure 3. Semi-quantitative reverse transcriptase polymerase chain reaction (RT-PCR) analyses of marmoset cytokine gene transcripts. $CD4^+$ (**A**) and $CD8^+$ cells (**C**) were isolated from marmoset spleens and stimulated in vitro with anti-CD3, anti-CD3/anti-CD28 or TSST-1, respectively. $CD4^+$ cells were prepared from peripheral blood (PB) of normal marmosets (**B**). H21 to H25 represent individual marmoset numbers. RNA was prepared from the cells and processed for RT-PCR. B lymphocytes were isolated from marmoset spleens using anti-human CD20 monoclonal antibody (mAb), and its RNA was used in parallel. The amplified fragments were quantified and shown as indexes calculated using the formula (cytokine/HPRT). HPRT = hypoxanthine-guanine phosphoribosyltransferase; IFN = interferon; IL = interleukin; TGF = transforming growth factor; TNF = tumor necrosis factor.

Figure 4. Insertion of *Alu*-like sequence into the marmoset *granzyme B* gene. (A) Alignment of *granzyme B* transcripts from human (Hs, NM_004131.3), chimpanzee (Pt, XM_509879.2) and common marmoset (Cj, EU918128.1). The 3′ portions of each transcript were aligned using the CLUSTALW tool. The common marmoset sequence indicated by bold, which does not have a counterpart in the transcripts from human and chimpanzee, is the Alu sequence. The termination codons of open reading flame (ORF) are indicated by underlines. Asterisks indicate identical residues. (B) Alignment of amino acid sequences of granzyme B proteins from human (NP_004122), chimpanzee (XP_509879), and common marmoset (EU918128). (C) Alignment of common marmoset-derived 317 nucleotide sequence (indicated by bold in panel A) with the human-derived *Alu-J* element.

human *Alu-J* element (Fig. 4C). Thus, the *Alu*-insertion into the ORF of *granzyme B* gene appears to be a feature unique to the common marmoset.

Detection of hematopoietic progenitor activity in marmoset bone marrow

CD117 and CD34 are the representative markers of murine and human hematopoietic progenitors, respectively. An extent of sequence conservation among the orthologous proteins of human, the common marmoset and mouse origin was examined by BLAST homology search (Table 1). The numbers therein represent the percentages of identical amino acid residues in three-way pair-wise comparisons. It can be seen that CD34 is relatively divergent among the three species, whereas CD117 is better conserved.

We then examined the activity of hematopoietic progenitors in marmoset bone marrow. Marrow cells were stained with anti-marmoset CD117 and CD34 mAbs (Fig. 5A). Four distinct fractions, namely $CD117^+CD34^+$, $CD117^+CD34^-$, $CD117^-CD34^+$, and $CD117^-CD34^-$, were detected. These anti-marmoset mAbs did not detect a positive population in human cord blood cells due to the lack of cross-reactivity with human antigens.

Using these mAbs, the four fractions described here were isolated from marmoset bone marrow cells by flow cytometry and assayed for their colony-forming activity in vitro. Human recombinant cytokines were added to the culture. Figure 5B shows the morphological appearance of burst-forming unit erythroid (BFU-E), colony-forming unit granulocyte (CFU-G), colony-forming unit macrophage (CFU-M), and colony-forming unit granulocyte-macrophage (CFU-GM) in the isolated $CD117^+CD34^+$ cells. At a level of microscopic resolution, these marmoset-derived colonies were indistinguishable from those of human and mouse. The

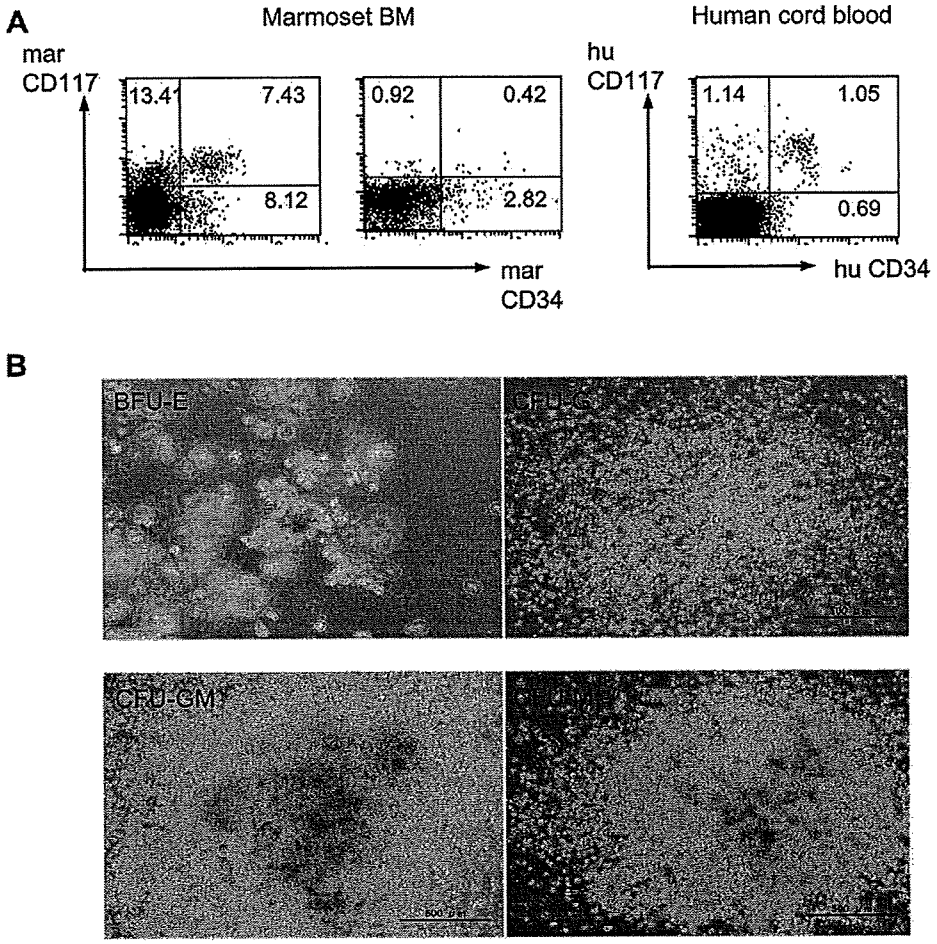

Figure 5. Hematopoietic progenitors in marmoset bone marrow as assayed in vitro. (**A**) Marmoset bone marrow (BM) cells and human cord blood cells were stained with the indicated monoclonal antibodies (mAbs), and their flow cytometrical patterns are displayed. The mAbs used were anti-marmoset CD117, anti-marmoset CD34, anti-human CD117, and anti-human CD34. (**B**) Morphological appearance of marmoset colonies formed in vitro. A $CD117^+CD34^+$ fraction was isolated from marmoset bone marrow, and assayed for colony-forming activity in the cytokine-supplemented culture. Phase contrast microscopic pictures are presented for burst-forming unit erythroid (BFU-E), colony-forming unit granulocyte (CFU-G), colony-forming unit macrophage (CFU-M), colony-forming unit granulocyte-macrophage (CFU-GM), respectively.

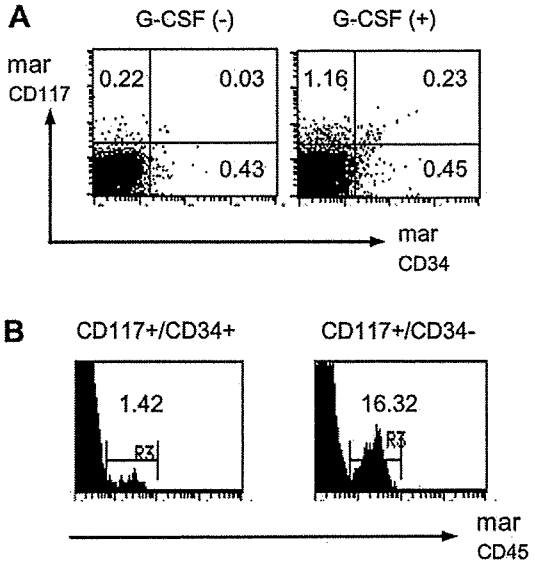

Figure 6. Hematopoietic progenitors in marmoset bone marrow as assayed in vivo. (**A**) Detection of peripherally mobilized progenitors in response to granulocyte colony-stimulating factor (G-CSF) injection. A marmoset individual was intravenously inoculated with human recombinant G-CSF, and peripheral blood was collected prior to (left panel) and 48 hours after the injection (right panel). Blood cells were stained using anti-marmoset CD117 and CD34 monoclonal antibodies (mAbs). (**B**) Lymphopoietic activity of marmoset progenitors as assayed in NOG mice. The $CD117^+CD34^+$ (left panel) and $CD117^+CD34^-$ (right panel) fractions isolated from marmoset bone marrow were inoculated into NOG mice, and 7 weeks after transplantation, peripheral blood was collected and stained using anti-marmoset CD45 mAb.

numbers of each colony were counted in each fraction and their average numbers are shown in Table 2. Quite similar numbers of colonies were formed from $CD117^+CD34^+$ and $CD117^+CD34^-$ fractions. However, only very weak colony-forming activity was detected for $CD117^-CD34^+$, and almost no activity for $CD117^-CD34^-$. This result suggests that hematopoietic activity as assayed in vitro resides mainly in the $CD117^+$ cells irrespective of CD34 expression.

Activity of marmoset hematopoietic progenitors as assayed in vivo

As described here, we could detect hematopoietic progenitors in marmoset bone marrow using marmoset-specific mAbs. Next, we examined the in vivo activity of marmoset progenitors. Human G-CSF was injected intravenously into marmosets. After 48 hours, peripheral blood was collected and stained with anti-marmoset mAbs (Fig. 6A). A $CD117^+$ fraction was not apparent in peripheral blood prior to G-CSF injection (left panel), but became evident after injection (right panel), corresponding to a sevenfold increase from 0.03% (left) to 0.23% (right). This indicates a mobilization of hematopoietic progenitors in response to G-CSF.

We also assayed the lymphopoietic activity of marmoset progenitors in vivo. For that, we used NOD/shi-SCID/IL-$2Rg^{null}$ (NOG) mice, a severe immunodeficient mouse cell line, because the mice have higher multipotential engraftment than any other mouse lines. The $CD117^+CD34^+$ and $CD117^+CD34^-$ fractions were isolated as mentioned here, and individually inoculated into NOG mice. After 7 weeks, peripheral blood was collected and stained for marmoset CD45 (Fig. 6B). In an individual inoculated with the $CD117^+CD34^-$ fraction, a substantial marmoset $CD45^+$ fraction emerged. In addition, the $CD20^+$ fraction was also observed in the $CD117^+CD34^-$-inoculated NOG mouse (data not shown). These observations indicate that the $CD117^+$ fraction developed into marmoset leukocytes, including a B-cell lineage, in vivo.

Discussion

In this study, to gain insight into how close or distant the immune system of the common marmoset is to that of humans and/or mice, we developed several mAbs directed toward marmoset antigens on T lymphocytes or on putative hematopoietic progenitors. CHO cells transfected with cDNAs and expressing marmoset proteins were initially used for screening the mAbs we produced against marmoset antigens. These cells were also used to examine the cross-reactivity of commercially available mAbs with human or mouse proteins. None of the examined anti-mouse mAbs showed any reactivity with marmoset antigens expressed on CHO cells, highlighting the great distance between marmoset and mouse epitopes. On the other hand, although mAbs against human CD34, CD45, and CD117 did not cross-react with respective marmoset antigens, other anti-human mAbs, including anti-CD4, anti-CD8, and anti-CD25 exhibited significant cross-reaction with the respective marmoset antigens. The reverse was not the case. The anti-marmoset CD4 or CD8 that we generated did not react with human CD4 or CD8. These observations suggest that use of anti-marmoset mAbs as was done in the present study would be ideal for examining marmoset immunity, although some anti-human mAbs could also be used as an alternative choice.

Marmoset $CD4^+$ T cells isolated from spleen cells and peripheral blood by using the established anti-marmoset mAbs showed various cytokine transcripts with TCR-mediated signaling. The induced cytokine transcripts included *IFN-γ*, *IL-4*, *IL-5*, *IL-10*, *IL-6*, and *IL-17*. These cytokines are produced from Th1, Th2, and Th17 T-cell subsets and play an important role in the immune response of humans and mice, suggesting that marmosets may have a similar immune function to humans. *TNF-α* and *TGF-β* transcripts were constitutively detected in marmoset $CD4^+$ cells even

prior to stimulation, which is not different from human and mouse. It must be emphasized that the present study established the authenticity of marmoset-derived cytokine transcripts because we designed the primers for PCR based on the marmoset sequences. On the other hand, the previous studies determined the marmoset cytokine transcripts by utilizing primers that were deduced by comparing the human and mouse orthologous genes [21,34]. Such an ambiguous method might allow the detection of only a few examples of cytokines.

TCR-stimulation caused an increment of *granzyme B* transcripts but not of *perforin 1* in these $CD8^+$ cells. In human, γδ T cells lose naïveness during childhood and start to express *perforin 1* constitutively [5,35]. Thus, one may speculate that the constitutive expression of *perforin 1* observed in the unstimulated marmoset $CD8^+$ T cells may not be detectable in resting cells but in already activated cells in some way. This is possible because the marmosets used were maintained under conventional, not pathogen-free, conditions. Alternatively, γδ T cells might be dominating in peripheral tissues of marmosets, which we could not yet determine as we have not cloned cDNA of any TCR chain genes, particularly γδ chains. Elucidation of this point requires development of anti-marmoset TCR γδ mAbs.

TSST-1 treatment of marmoset $CD4^+$ T cells enhanced their CD25 expression, reflecting the fact that CD25 expression is induced through the TCR-coupled activation process. To be noted is the existence of a $CD25^+$ subfraction in the freshly isolated splenic $CD4^-$ cells as well as $CD4^+$ T cells. The latter cells could be activated ones because they are maintained in non-specific pathogen free (SPF) environment as described here. Of a $CD4^-CD25^+$ fraction, they belong to non-T cells such as B cells and DCs, as shown in the past reports that these cells in human and mouse are induced to express CD25 if they are activated. In mouse and human, a $CD4^-CD25^+$ $CD20^+$ phenotype has been reported to represent B cells [36,37]. Further analyses of CD25 expression in marmoset resting B cells are required, particularly for developmental genetics/ biology.

We generated and utilized anti-marmoset CD117 and CD34 mAbs for hematopoietic analysis. The percentage of $CD117^+CD34^+$ fraction was significantly increased in peripheral blood of marmosets receiving human G-CSF injection. These $CD117^+CD34^+$ cells exhibited multidifferentiating capabilities into myeloid and erythroid lineages by in vitro colony-forming assays. Furthermore, these double-positive cells, when transplanted into NOG mice, generated $CD45^+$ cells. Therefore, the $CD117^+CD34^+$ fraction most likely contains hematopoietic progenitor activity. The marmoset $CD34^+$ fraction reported to possess colony-forming activity [29] might have contained $CD117^+$ cells. In fact, as seen in Table 2, $CD117^+$ cells with and without CD34 expression showed higher hematopoietic activity than $CD117^-$ cells, while human $CD34^-CD117^+$ cells are reported to differentiate mainly to erythroid lineage cells [38]. A human $CD34^+$ fraction has been reported to possess progenitor activity into various cell lineages, including lymphocytes and DCs [39–41]. However, $CD34^+CD117^-$ cells are reported to possess less multipotentiality [41]. In mice, hematopoietic progenitor activity is present in $CD34^-CD117^+SCA\text{-}1^+$ cells [42,43]. Therefore, the previously known markers for hematopoietic progenitors may vary from species to species. The details of whether marmoset progenitors are more alike to mouse or human have to be investigated in greater detail.

In summary, the cell and cytokine profiles seen in marmoset helper and killer T cells were essentially reminiscent of those in human and mouse. Several marmoset antigens showed cross-reactivity with anti-human mAbs, suggesting a closer relationship of marmoset to human. The development of sophisticated analytical tools including mAbs should eventually contribute to the establishment of marmoset hematopoietic and immune systems as a human model.

Acknowledgments

We thank Dr. Hideki Kato, Hamamatsu Medical University (Shizuoka, Japan) for helpful discussions and for providing blood of common marmosets. We also thank Dr. Shuji Takabayashi, Fumika Toyota, and members of The Institute for Experimental Animals (Kanagawa, Japan) for help in collecting and shipping samples. This work was supported by a research grant from Japan Science Promotion (Tokyo, Japan) to S.H.

Conflict of Interest Disclosure

No financial interest/relationships with financial interest relating to the topic of this article have been declared.

References

1. Rautajoki K, Kylaniemi M, Raghav S, Rao K, Lahesmaa R. An insight into molecular mechanisms of human T helper cell differentiation. Ann Med. 2008;40:322–335.
2. Mestas J, Hughes C. Of mice and not men: differences between mouse and human immunology. J Immunol. 2004;172:2731–2738.
3. Shortman K, Liu Y-J. Mouse and human dendritic cell subtypes. Nat Rev Immunol. 2002;2:151–161.
4. Karaghiosoff M, Neubauer H, Lassnig C, et al. Partial impairment of cytokine responses in Tyk2-deficient mice. Immunity. 2000;13: 549–560.
5. De Rosa S, Andrus J, Perfetto S, et al. Ontogeny of gd T cells in humans. J Immunol. 2004;172:1637–1645.
6. Martin A, Valentine M, Unger P, Yeung S, Shults L, Davies T. Engraftment of human lymphocytes and thyroid tissue into scid and rag2-deficient mice: absent progression of lymphocytic infiltration. J Clin Endocrinol Metabol. 1994;79:716–723.
7. Pflumio F, Izac B, Katz A, Shultz L, Vainchenker W, Coulombel L. Phenotype and function of human hematopoietic cells engrafting immune-deficient CB17-severe combined immunodeficiency mice and nonobese diabetic-severe combined immunodeficiency mice after transplantation of human cord blood mononuclear cells. Blood. 1996; 88:3731–3740.

8. van der Loo J, Hanenberg H, Cooper R, Luo F-Y, Lazaridis E, Williams D. Nonobese diabetic/severe combined immunodeficiency (NOD/S-CID) mouse as a model system to study the engraftment and mobilization of human peripheral blood stem cells. Blood. 1998;92:2556–2570.
9. Roncarolo M, Carballido J, Rouleau M, Namikawa R, de Vries J. Human T-and B-cell functions in SCID-hu mice. Semin Immunol. 1996;8:207–213.
10. McCune J, Namikawa R, Kaneshima H, Shultz L, Lieberman M, Weissman I. The SCID-hu mouse: murine model for the analysis of human hematolymphoid differentiation and function. Science. 1988; 241:1632–1639.
11. Novelli E, Ramirez M, Leung W, Civin C. Human hematopoietic stem/progenitor cells generate CD5+ B lymphoid cells in NOD/SCID mice. Stem Cells. 1999;17:242–252.
12. Ito M, Hiramatsu H, Kobayashi K, et al. NOD/SCID/gamma(c)(null) mouse: an excellent recipient mouse model for engraftment of human cells. Blood. 2002;100:3175–3182.
13. Ito M, Kobayashi K, Nakahata T. NOD/Shi-scid IL2rgamma(null) (NOG) mice more appropriate for humanized mouse models. Curr Top Microbiol Immunol. 2008;324:53–76.
14. Kametani Y, Shiina M, Katano I, et al. Development of human-human hybridoma from anti-Her-2 peptide-producing B cells in immunized NOG mouse. Exp Hematol. 2006;34:1240–1248.
15. Matsumura T, Kametani Y, Ando K, et al. Functional CD5+ B cells develop predominantly in the spleen of NOD/SCID/gammac(null) (NOG) mice transplanted either with human umbilical cord blood, bone marrow, or mobilized peripheral blood CD34+ cells. Exp Hematol. 2003;34:1240–1248.
16. Saito Y, Kametani Y, Hozumi K, et al. Reconstitution of functional human B lymphocytes in NOD/SCID mice engrafted with ex vivo expanded CD34(+) cord blood cells. Int Immunol. 2002;30:1036–1043.
17. Ito R, Shiina M, Saito Y, Tokuda Y, Kametani Y, Habu S. Antigen-specific antibody production of human B cells in NOG mice reconstituted with the human immune system. Curr Top Microbiol Immunol. 2008;324:95–107.
18. Mansfield K. Marmoset models commonly used in biomedical research. Comp Med. 2003;53:383–392.
19. Mansfield K, Tardif S, Eichler E. White paper for complete sequencing of the common marmoset (Callithrix jacchus). 2004. Available at: http://www.genome.gov/Pages/Research/Sequencing/SeqProposals/MarmosetSeq.pdf. Accessed September 18, 2009.
20. Hibino H, Tani K, Ikebuchi K, et al. The common marmoset as a target preclinical primate model for cytokine and gene therapy studies. Blood. 2008;93:2839–2848.
21. Genain C, Abel K, Belmar N, et al. Late complications of immune deviation therapy in a nonhuman primate. Science. 1996;274:2054–2057.
22. Genain C, Hauser S. Experimental allergic encephalomyelitis in the new world monkey Callithrix jacchus. Immunol Rev. 2001;183:159–192.
23. LaBonte J, Babcock G, Patel T, Sodroski J. Blockade of HIV-1 infection of new world monkey cells occurs primarily at the stage of virus entry. J Exp Med. 2002;431:431–445.
24. Einspanier A, Lieder K, Bruns A, Husen B, Thole H, Simon C. Induction of endometriosis in the marmoset monkey (Callithrix jacchus). Mol Hum Reprod. 2006;12:291–299.
25. Massacesi L, Genain C, Lee-Parritz D, Letvin N, Canfield D, Hauser S. Active and passively induced experimental autoimmune encephalomyelitis in common marmosets: a new model for multiple sclerosis. Ann Neurol. 1995;37:519–530.
26. 't Hart B, Laman J, Bauer J, Blezer E, van Kooyk Y, Hintzen R. Modelling of multiple sclerosis: lessons learned in a non-human primate. Lancet Neurol. 2004;3:588–597.
27. Sasaki E, Suemizu H, Shimada A, et al. Generation of transgenic non-human primates with germline transmission. Nature. 2009;459:515–516.
28. Kohu K, Yamabe E, Matsuzawa A, et al. Comparison of 30 immunity-related genes from the common marmoset with orthologues from human and mouse. Tohoku J Exp Med. 2008;215:167–180.
29. Izawa K, Tani K, Nakazaki Y, et al. Hematopoietic activity of common marmoset CD34 cells isolated by a novel monoclonal antibody MA24. Exp Hematol. 2004;32:843–851.
30. Brok H, Hornby R, Griffiths G, Scott L, Hart B. An extensive monoclonal antibody panel for the phenotyping of leukocyte subsets in the common marmoset and the cotton-top tamarin. Cytometry. 2001;45: 294–303.
31. Marchler-Bauer A, Anderson J, Cherukuri P, et al. CDD: a conserved domain database for protein classification. Nucleic Acids Res. 2005; 33:192–196.
32. Song Y, Liu F, Zhang G, Liu D. Hydrodynamics-based transfection: simple and efficient method for introducing and expressing transgenes in animals by intravenous injection of DNA. Methods Enzymol. 2002; 246:92–105.
33. Ito R, Maekawa S, Kawai K, et al. Novel monoclonal antibodies recognizing different subsets of lymphocytes from the common marmoset (Callithrix jacchus). Immunol Lett. 2008;121:116–122.
34. McFarland H, Lobito A, Johnson M, et al. Effective antigen-specific immunotherapy in the marmoset model of multiple sclerosis. J Immunol. 2001;166:2116–2121.
35. Accardo-Palumbo A, Ferrante A, Cadelo M, et al. The level of Granzyme A is elevated in the plasma and in the Vgamma9/Vdelta2 T cell culture supernatants with active Behger's disease. Clin Exp Rheumatol. 2004;22(Suppl 34):S45–S49.
36. Amu S, Tarkowski A, Dorner T, Bokarewa M, Brisslert M. The human immunomodulatory CD25+ B cell population belongs to the memory B cell pool. Scand J Immunol. 2007;66:77–86.
37. Brisslert M, Bokarewa M, Larsson P, Wing K, Collins L, Tarkowski A. Phenotypic and functional characterization of human CD25+ B cells. Immunology. 2006;117:548–557.
38. Papayannopoulou B, Brice M, Broudy V, Zsebo K. Isolation of c-kit receptor-expressing cells from bone marrow, peripheral blood, and fetal liver: functional properties and composite antigenic profile. Blood. 1991;78:1403–1412.
39. Hogan C, Shpall E, McNulty O, et al. Engraftment and development of human CD34(+)-enriched cells from umbilical cord blood in NOD/LtSz-scid/scid mice. Blood. 1997;90:85–96.
40. Greiner D, Hesselton R, Shultz L. SCID mouse models of human stem cell engraftment. Stem Cells. 1998;16:166–177.
41. Wermann K, Fruehauf S, Haas R, Zeller W. Human-mouse xenografts in stem cell research. J Hematother. 1996;5:379–390.
42. Galy A, Morel F, Hill B, Chen B. Hematopoietic progenitor cells of lymphocytes and dendritic cell. J Immunother. 1998;21:132–141.
43. Okada S, Nakauchi H, Nagayoshi K, Nishikawa S, Miura Y, Suda T. In vivo and in vitro stem cell function of c-kit- and Sca-1-positive murine hematopoietic cells. Blood. 1992;80:3044–3050.

Vaccine 27 (2009) 7116–7124

Contents lists available at ScienceDirect

Vaccine

journal homepage: www.elsevier.com/locate/vaccine

A genetically engineered adenovirus vector targeted to CD40 mediates transduction of canine dendritic cells and promotes antigen-specific immune responses *in vivo*

Erin E. Thacker[a], Masaharu Nakayama[a], Bruce F. Smith[g,h], R. Curtis Bird[h], Zhanat Muminova[e], Theresa V. Strong[c,d,e], Laura Timares[c,f], Nikolay Korokhov[i], Ann Marie O'Neill[g], Tanja D. de Gruijl[j], Joel N. Glasgow[a,b,d], Kenzaburo Tani[k], David T. Curiel[a,c,d,*]

[a] *Division of Human Gene Therapy, Departments of Medicine, Obstetrics and Gynecology, Pathology, Surgery, Birmingham, AL 35294, United States*
[b] *Division of Cardiovascular Disease, University of Alabama at Birmingham, Birmingham, AL 35294, United States*
[c] *Comprehensive Cancer Center, University of Alabama at Birmingham, Birmingham, AL 35294, United States*
[d] *Gene Therapy Center, University of Alabama at Birmingham, Birmingham, AL 35294, United States*
[e] *Division of Hematology/Oncology, Department of Medicine, University of Alabama at Birmingham, Birmingham, AL 35294, United States*
[f] *Department of Dermatology, The UAB Skin Diseases Research Center, University of Alabama at Birmingham, Birmingham, AL 35294, United States*
[g] *Scott-Ritchey Research Center, Auburn University, Auburn, AL 36849, United States*
[h] *Department of Pathobiology, Auburn University, Auburn, AL 36849, United States*
[i] *VectorLogics, Inc., Birmingham, AL 35294, United States*
[j] *Division of Immunotherapy, Department of Medical Oncology, VU University Medical Center, Amsterdam, The Netherlands*
[k] *Division of Molecular and Clinical Genetics, Medical Institution of Bioregulation, Kyushu University, Fukuoka, Japan*

ARTICLE INFO

Article history:
Received 26 August 2008
Received in revised form 2 September 2009
Accepted 16 September 2009
Available online 26 September 2009

Keywords:
Cancer immunotherapy
Adenovirus
Dendritic cell
Dog
Vaccine

ABSTRACT

Targeting viral vectors encoding tumor-associated antigens to dendritic cells (DCs) *in vivo* is likely to enhance the effectiveness of immunotherapeutic cancer vaccines. We have previously shown that genetic modification of adenovirus (Ad) 5 to incorporate CD40 ligand (CD40L) rather than native fiber allows selective transduction and activation of DCs *in vitro*. Here, we examine the capacity of this targeted vector to induce immune responses to the tumor antigen CEA in a stringent *in vivo* canine model. CD40-targeted Ad5 transduced canine DCs via the CD40-CD40L pathway *in vitro*, and following vaccination of healthy dogs, CD40-targeted Ad5 induced strong anti-CEA cellular and humoral responses. These data validate the canine model for future translational studies and suggest targeting of Ad5 vectors to CD40 for *in vivo* delivery of tumor antigens to DCs is a feasible approach for successful cancer therapy.

1. Introduction

Many immunological features of cancers that allow evasion of immune surveillance and destruction have been revealed, enabling the development of new and more effective immunotherapeutic strategies. Immune evasion is now recognized to be due primarily to a breakdown in the normal route of tumor antigen presentation to T cells [1]. In order to mount an immune response against a tumor, antigen presenting cells (APCs) monitoring peripheral tissues must present tumor-associated antigens (TAA) to T cells. In a fully functional immune system, APCs capture and present TAA to CD8+ T cells (lymphocytes) (CTL) and CD4+ helper T (Th) cells in lymph nodes (LN), leading to the expansion and activation of antigen-specific effector T cells. Once activated, CTLs recognize tumor cells expressing the presented TAA. The identification of a variety of cancer-specific TAA has provided more options for immunotherapy; however, TAA are often self-antigens to which a considerable immunological tolerance is maintained, especially depending on the route of T cell presentation [2]. Therefore, strategies for overcoming tolerance and generating effective immune responses against TAA are being developed based on harnessing the immunostimulatory activity of APCs.

Delivering TAA specifically to dendritic cells (DCs) with an antigen-delivery system offers tremendous potential for the development of new cancer vaccines [3]. Supporting this, pre-clinical and clinical trials have focused on adoptive transfer of TAA-exposed DCs. These approaches involve isolating DCs from the blood of patients, exposing the DCs to TAA and other maturation stimuli in

* Corresponding author at: University of Alabama at Birmingham, 901 19th Street South BMR2-508, Birmingham, AL 35294-2172, United States. Tel.: +1 205 934 8627; fax: +1 205 975 7476.
E-mail address: curiel@uab.edu (D.T. Curiel).

0264-410X/$ – see front matter © 2009 Elsevier Ltd. All rights reserved.
doi:10.1016/j.vaccine.2009.09.055

culture, and finally, re-injecting them into the patient. Although encouraging results have been reported, there are substantial medical, economic, and logistic complexities to this approach. In addition, while pre-clinical trials in mice demonstrated highly promising immune responses, including tumor regression and remission, clinical trials in humans resulted in far fewer cases of tumor stability or regression, suggesting these vaccines are not yet optimal [4–8]. Possibly underlying these results, recent evidence indicates that DCs matured *ex vivo* do not accurately mimic DCs matured *in vivo*, precluding optimal immune system stimulation [9]. Thus, a strategy to facilitate DC transduction to mediate TAA delivery *in vivo* that is universally efficacious, regardless of haplotype, is required.

In regard to DC transduction efficiency, gene transfer and immune stimulation, viral transduction methods have been found to be superior to non-viral methods [10–12]. In addition to high gene transfer efficiency, transduction of DCs with adenovirus serotype 5 (Ad5)-based vectors offers many benefits over other viral vectors. Ad5-mediated transduction does not require cell proliferation and poses a low risk for insertional mutagenesis [13–16]. Furthermore, non-replicating Ads provide the additional benefit of delivering TAA for only a finite amount of time, thus minimizing the chances of inducing hyporesponsiveness to chronic antigen presentation. Despite these advantages, DCs are relatively refractory to Ad5 transduction due to limited cell surface expression of the primary Ad5 receptor, coxsackie virus and adenovirus receptor (CAR) [17]. Thus, efficient Ad5-mediated gene transfer to DCs requires high multiplicities of infection (MOI). To overcome this, our lab has re-targeted Ad5 to CD40 expressed on cell surfaces, achieving efficient and specific DC transduction and antigen-specific immune responses using low doses of Ad5 administered subcutaneously, a site enriched for DCs [17–25]. In addition to providing a means for efficient DC transduction, CD40 ligation and activation induces migration of mature DCs to the T cell populated areas of the draining lymph node, thus CD40-targeted vectors are likely to provide additional immunotherapeutic benefits.

In the experiments presented here, the transduction potential of CD40-targeted Ad5 was determined in canine DCs, and the immunostimulatory capacity of this targeting strategy was evaluated in dogs, the most relevant translational animal model available for evaluating many therapeutic modalities designed to combat human diseases. Of particular relevance to our studies, dogs are naturally susceptible to several cancers which mimic the onset, progression and symptoms of the corresponding human cancers, allowing therapeutic evaluation with increased clinical relevance [26–29]. Indeed, many advances in human cancer therapies have been made or improved through studies in canine patients, including the first evaluations of cancer vaccines, and the analysis of cytokine and chemotherapeutic regimens for pulmonary metastases [26]. In addition, canine models provide dosing and vector production challenges similar to those encountered in human clinical trials [26,30,31].

The data presented from this pilot study in healthy dogs validate the utility of the canine model for our translational studies, and suggest that specific targeting of Ad5 vectors to DCs for *in vivo* delivery of genes encoding TAA may provide an enhanced immune response to disease-related antigens.

2. Materials and methods

2.1. Cell lines

The human embryonic kidney cell line 293 was purchased from Microbix (Toronto, Ontario, Canada). The 293F28 and 293/hCD40 cell lines are derivatives of 293 cells which express either Ad5 wild-type fiber (for mosaic virus propagation as described below) or human CD40 as previously described [21]. The 293/cCD40 cell line is a derivative of the 293 cell line which expresses canine CD40, and was generated by transfection of 293 cells with the plasmid pcDNA3.1canineCD40, and subsequent selection with 1000 μg/ml of Geneticin (G418). A cell clone derived from this population that expressed high levels of canine CD40 was identified by RT-PCR. All 293 and 293-derived cell lines were propagated in a 50:50 mixture of Dulbecco's modified Eagle's medium and Ham's F-12 medium (DMEM/F-12) supplemented with 10% (v/v) fetal calf serum (FCS), L-glutamine (2 mM), penicillin (100 units/ml) and streptomycin (100 μg/ml). FCS was purchased from Gibco-BRL (Grand Island, NY) and media and supplements were from Mediatech (Herndon, VA). RT-PCR analysis of cell lines revealed 4.47×10^7 copies/μg of human CD40 mRNA in 293/hCD40 compared to 5.6×10^{-2} copies/μg in control 293 cells, and 6.44×10^3 copies/μg of canine CD40 mRNA in 293/cCD40 cells. 293F28 cells were maintained with 100 μg/ml Zeocin (Invitrogen), and 293/hCD40 and 293/cCD40 cells were maintained with 100 μg/ml G418. All cell lines were cultured at 37 °C in 5% CO_2.

2.2. Gene therapy vectors

Ad5.FFhCD40L vectors expressing artificial fiber proteins containing FF-CD40L and encoding either luciferase, CEA or GFP/CEA were constructed as previously described [20,21]. Ad5 vectors expressing the native fiber protein and encoding either luciferase, GFP/luciferase or CEA were employed as controls [20,32,33]. Briefly, Ad5 vectors encoding the native fiber protein were generated by transfection of 293 cells with Pac I-digested Ad rescue vectors. Vectors with FF-CD40L were generated by transfection of 293F28 cells with Pac I-digested Ad rescue vectors. 293F28 cells stably express the native Ad5 fiber, thus viruses rescued at this point were mosaic in the sense that the Ad5 virions randomly incorporated a mixture of native fibers and FF-CD40L chimeras. After additional rounds of amplification on 293F28 cells, the viruses were amplified in 293 cells, which do not express native Ad5 fiber, to obtain virus particles containing only FF-CD40L [21].

All Ad5 vectors were isolated from infected cells and purified by equilibrium centrifugation in CsCl gradients according to a standard protocol [34]. The protein concentrations in the viral preparations were determined using the DC protein assay (BioRad, Hercules, CA) with purified bovine serum albumin (BSA) as a standard. The virus titers were calculated using the formula: 1 μg of protein = 4×10^9 viral particles (vp).

2.3. Preparation of canine peripheral blood mononuclear cell populations

Whole blood (40–60 ml) was collected from normal outbred dogs in EDTA tubes (Becton, Dickinson), gently and thoroughly mixed and centrifuged 30 min at 1000 × *g* at RT. The buffy coat containing the peripheral blood mononuclear cell (PBMC) population was extracted with a pipette in 1–2 ml and diluted with 8 ml HBS (HEPES-buffered saline, no Mg/Ca, Gibco/BRL). The cell suspension was layered over 5 ml Histopaque 1077 (Sigma–Aldrich) and centrifuged at 1000 × *g* at RT for 30 min. The band containing the PBMC population was extracted in 1–2 ml into a new sterile tube and diluted with 2 ml HBS, mixed, and centrifuged once more. The supernatant was removed and the cells gently resuspend in 5 ml HBS. The cells were centrifuged once more and resuspended in 4 ml flow wash buffer (FWB–HBS containing 10% fetal bovine serum) and incubated at RT at least 40 min to allow blocking of nonspecific sites.

2.4. Flow cytometry and fluorescent activated cell sorting for canine dendritic cells

Antibodies were obtained that recognize canine CD11c (monoclonal mouse anti-dog CD11c, Serotec) and human CD40 (monoclonal mouse clone B-B20, prelabeled with Zenon reagent PE/Alexa Fluor 610, Invitrogen). The PBMC suspension was centrifuged at 200 × *g* at RT for 10 min, the supernatant removed, and the cells resuspended in 1 ml FWB. Primary antibodies (100 μl each) were then added, gently mixed, and incubated for 60 min at RT in the dark. Then, 2 ml HBS was added and the cell suspension centrifuged at 200 × *g* for 10 min. The supernatant was aspirated and the cells were washed two additional times in 2 ml HBS, finally resuspending them in 1 ml FWB. Each cell suspension was filtered to 50 μm in a sterile CellTrics disposable filter (Partec, Germany).

Flow cytometry assays and fluorescent activated cell sorting (FACs) were performed on a MoFlo flow cytometer and cell sorter (Beckman Coulter). The CD11c expression profiles were determined using Summit 4.0 software (Beckman Coulter). The entire cell suspension was sorted for each experiment and sorted cells (CD11c+ and CD11c−) sterilely collected into tubes containing 1 ml of FBS. Both samples and sorted populations of cells were maintained at RT during the entire process.

To ensure recovery of exposed CD40 on the cell surface, cells were allowed to recover for 4 h prior to transduction with Ad vectors. Following transduction, cells were collected by centrifugation, and brought into culture in RPMI-1640 (Gibco/BRL) containing 10% FBS, penicillin/streptomycin/fungizone (Gibco/BRL) and 25% lymphocyte conditioned media (CM). CM was obtained from cultures of freshly prepared canine lymphocytes which had been stimulated for 24–48 h with phytohemagglutinin (PHA, 10 μg/ml, Sigma–Aldrich) [35,36].

2.5. Recombinant protein purification and western blot analysis

The 6-HIS-tagged soluble human CD40L protein and its derivatives were expressed in *Escherichia coli* BL21(DE3)(pLysS) as previously described [21]. The concentrations of the proteins in purified preparations and in cell lysate were determined using the BioRad DC protein assay.

2.6. Gene transfer experiments

293, 293/hCD40 and 293/cCD40 cell lines and canine DCs were plated in 24-well plates at 1×10^5 cells/well. Prior to transduction, cells were washed with serum-free growth medium and incubated on ice with 0.2 ml of either medium or medium containing a blocking agent. In the latter instance, recombinant Ad5 fiber knob [37] or soluble hCD40L proteins were added to the medium at concentrations of 100 μg/ml for 1 h on ice. Cells were transduced at a multiplicity of infection (MOI) of 10, 100 or 1000 vp per cell with Ad5 vectors in medium containing 2% FCS. After incubation on ice for 1 h, the medium containing the virus and the inhibitor was removed, and cells were washed with medium containing 10% FCS. Fresh medium was added, and incubation was continued at 37 °C for 22 h to allow reporter gene expression. Cells were then washed with PBS and lysed in Luciferase Reporter Lysis Buffer (Promega). The luciferase activity in the cell lysates was measured according to the manufacturer's protocol. Each data point was assessed in triplicate and calculated as the mean of three determinations. In instances where transduction was performed without the addition of a blocking agent, the virus was added to the cells in 0.4 ml aliquots of medium containing 2% FCS.

All incubation and washing steps in gene transfer experiments involving DCs were performed in cell suspensions since these cells are only loosely adherent. To minimize variation in the data, which could result from the loss of cells during the washing steps, the luciferase activity measured in the cell lysates was normalized to the protein concentration of resulting cell lysates.

2.7. In vivo canine vaccinations

All experiments were conducted under the oversight of the Auburn University IACUC committee in AAALAC approved animal and clinical care facilities. Outbred beagle dogs from two litters were used for vaccination. The dogs were 10 and 15 weeks of age at the start of the experiment and weighed approximately 10–15 kg each. Additional adult beagle and beagle-corgi crosses were used to provide blood for isolation of PBMCs. 1×10^9 vp of Ad5CEA.FF/hCD40L (five dogs) or control Ad5CEA (five dogs) vectors were delivered in 0.5 ml sterile phosphate-buffered saline (PBS) to each dog. Intradermal (i.d.) injections were performed in the right lower abdomen using a 25 gauge needle. The dogs were re-injected with the same dose of each Ad5 vector and by the same route as their original injection on weeks 4, 8 and 12. Peripheral blood was collected each week and used for ELISA detection of anti-CEA antibodies. At week 14, lymphocytes were purified from collected peripheral blood for lymphoproliferation assays.

2.8. Lymphoproliferation assays

PBMCs were obtained by density gradient centrifugation using lymphocyte separation media (Cellgro, Mediatech, Inc, Herndon, VA) and were resuspended in complete medium consisting of RPMI 1640 supplemented with 10% fetal bovine serum, 2 mM L-glutamine, 50 μM 2-mercaptoethanol, and antibiotics. Cells were added at 1×10^5 cells per well in round bottom 96-well plates. Stimulated cells were incubated in triplicate wells with recombinant human CEA protein (Vitro Diagnostics, Inc. Aurora, CO) over a range of concentrations (1–30 μg/ml). Additionally, BSA (30 μg/ml) or ovalbumin (OVA) (25 μg/ml) wells were included as negative control antigens and Con-A wells (0.5 μg/ml) were included as positive control mitogens. Control cells were cultured in complete medium alone. All cells were incubated at 37 °C in a humidified atmosphere of 5% CO_2 in air for two days, followed by an overnight pulse with 1 μCi/well of tritiated thymidine diluted at 50 μCi/ml. Cells were harvested and incorporated radioactivity was quantified using a solid-phase beta scintillation counter (Matrix 9600; Packard Instrument Co., Downers Grove, IL). The Stimulation Index (S.I.) was calculated as the mean counts per million (cpm) of the stimulated cells divided by the mean cpm of the control (OVA-stimulated) cells. A positive response was defined as a post-vaccination S.I. >3.0. The assay was performed in triplicate for each sample and results are presented as means.

2.9. ELISA for detection of anti-CEA antibodies

For CEA antibody detection, 96-well EIA plates (Costar 3590) were coated with recombinant CEA protein (Vitro Diagnostics, Inc. Aurora, CO) at 100 ng/well in borate saline (BS) buffer, pH 8.4, for 4 h at RT, and then blocked with borate saline plus 1% (w/v) bovine serum albumin (BS-BSA). Serial three-fold dilutions of dog serum in BS-BSA (1:50–1:109,350) were added to the wells and incubated overnight at 4 °C. Plates were washed with PBS containing 0.05% (v/v) Tween-20 and incubated with AP conjugated rabbit anti-dog (IgG H+L) antibodies (Jackson Immunoresearch Laboratories, Inc. West Grove, PA) diluted 1:2000 in BS-BSA for 4 h at RT. After washing, AP substrate (*p*-nitrophenyl phosphate, Sigma St. Louis, MO) in diethanolamine buffer, pH 9.0, was added and incubated for 20 min at RT. Absorbance was measured at 405 nm on

a Multiskan Ascent microplate reader using Ascent software (Labsystems OY, Helsinki, Finland). Absorbance on CEA coated plates was corrected for absorbance on parallel plates coated with ovalbumin (Sigma–Aldrich Chemical Co., St. Louis, MO). COL-1 mouse monoclonal antibody to CEA (NeoMarkers, Fremont, CA) followed with AP conjugated goat anti-mouse IgG (Southern Biotechnology, Birmingham, AL) was used as a positive control. For detection of IgG isotypes goat anti-dog IgG1 and sheep anti-dog IgG2 antibodies conjugated to horseradish peroxidase (Bethyl Laboratories Inc., Montgomery, TX) were applied to the wells at a dilution of 1:10,000. After incubation and wash 3,3′, 5′5 tetramethyl benzidine substrate (Sigma) was applied for colorimetric development. The reaction was stopped by adding 0.5 M H_2SO_4 and absorbance was read at 450 nm. Statistical analysis was performed by using two-tailed Student's *t*-test and values are presented as mean ± standard error of the mean.

3. Results

3.1. Generation of CD40-targeted Ad5

Human, rhesus and murine DCs have been successfully transduced with CD40-targeted Ad5 *in vitro*, resulting in selective transduction and simultaneous activation of DCs, indicating CD40 is an effective target in many species [17–24,38,39]. To establish the principle that CD40-targeted Ad5 can also mediate gene transfer to canine DCs, we employed a genetically engineered Ad5 vector encoding firefly luciferase, designated Ad5Luc.FF/hCD40L (Fig. 1) [19,21]. This vector was previously constructed so that the shaft and knob domains of the native fiber protein are replaced by phage T4 fibritin (as a trimerization motif) genetically fused to the TNF-Like (TNF-L) ectodomain of human CD40L (Fig. 1A). The presence of the phage T4 fibritin structure allows the TNF-L ectodomain of CD40L to retain its functional tertiary structure, required for activation of CD40 [21]. Human and canine CD40 are 83% similar, and amino acids predicted to be involved in CD40-CD40L binding are conserved [40,41], suggesting an Ad5 vector expressing human CD40L may interact effectively to allow transduction of CD40-expressing canine cells.

3.2. Gene transfer analysis in 293 cells expressing CD40

To confirm that the human CD40L ectodomain of Ad5Luc.FF/hCD40L mediates vector targeting to canine CD40, luciferase transgene expression was analyzed as a measure of vector transduction potential in 293 cells and cell lines stably

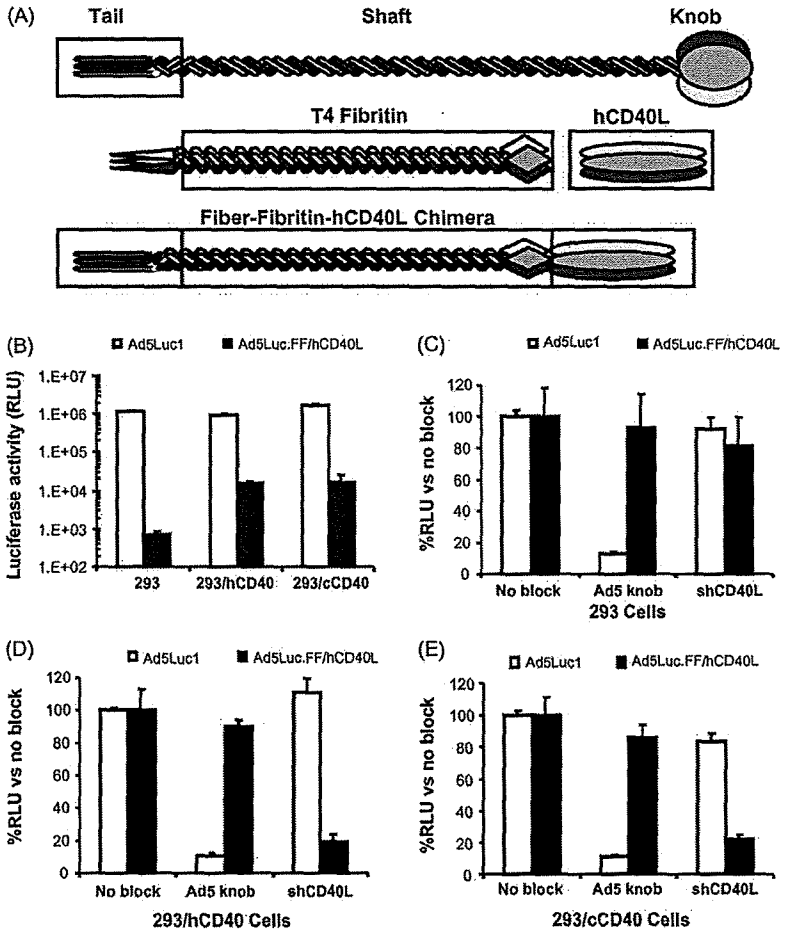

Fig. 1. Efficiency of gene transfer and receptor specificity of CD40-targeted Ad5. (A) Schematic diagram of CD40-targeted Ad5. The shaft and knob domains of native Ad5 fiber were replaced by phage T4 fibritin genetically fused to the TNF-L ectodomain of human CD40L. (B) 293, 293/hCD40 and 293/cCD40 cells were transduced with untargeted Ad5Luc1 (white bars) or CD40-targeted Ad5Luc.FF/hCD40L (black bars) at an MOI of 10 vp/cell. To determine receptor specificity, 293 (C), 293/hCD40 (D) and 293/cCD40 (E) cells were transduced with untargeted Ad5Luc1 (white bars) or CD40-targeted Ad5Luc.FF/hCD40L (black bars) at an MOI of 10 vp/cell. Prior to infection with virus, cells were incubated with recombinant Ad5 fiber knob or shCD40L to block transduction through CAR or CD40, respectively. 24 h after transduction, luciferase activity was determined as a measure of Ad5-mediated gene transfer. Luciferase activity is expressed as relative light units. Luciferase activity detected in the presence of blocking agents is normalized against luciferase activity in absence of blocking agents. Mean ± SD are shown from three replicates performed simultaneously.

expressing CD40. 293 cells, which do not express endogenous CD40, or 293 cells stably transfected with either human CD40 (293/hCD40) or canine CD40 (293/cCD40) were incubated with either untargeted Ad5Luc1 or CD40-targeted Ad5Luc.FF/hCD40L (10 vp/cell) (Fig. 1B). All 293 cell lines, which express the Ad5 receptor, CAR, were efficiently transduced by untargeted Ad5Luc1. In contrast, wild-type 293 cells incubated with Ad5Luc.FF/hCD40L expressed very low levels of luciferase, indicating this CD40-targeted vector does not transduce cells efficiently through CAR. However, Ad5Luc.FF/hCD40L-mediated luciferase expression in both 293/hCD40 and 293/cCD40 cells (Fig. 1B), suggesting Ad5Luc.FF/hCD40L capably transduces cells expressing either human or canine CD40.

3.3. Validation of CD40-mediated transduction

To further investigate the targeting specificity of Ad5Luc.FF/hCD40L, viral transduction was performed in the presence of specific blocking agents. Prior to transduction, 293, 293/hCD40 and 293/cCD40 cells were incubated with either soluble recombinant Ad5 fiber knob or soluble human CD40L (shCD40L) to block CAR or CD40, respectively, on the cell surface. Luciferase expression under these blocking conditions was compared to luciferase expression without blocking (normalized for each vector to 100%). As shown in Fig. 1(C–E), transduction of all 293 cell lines by Ad5Luc1 was inhibited by soluble knob (87% block in 293 cells, and 90% block in 293/hCD40 and 293/cCD40), indicating transduction by untargeted Ad5 requires CAR, as expected. The very low level of luciferase expression in 293 cells incubated with Ad5Luc.FF/hCD40L was not affected by soluble Ad5 knob (Fig. 1C). The high luciferase expression levels in 293/hCD40 and 293/cCD40 cells transduced by Ad5Luc.FF/hCD40L were not affected when CAR was blocked with soluble Ad5 knob (Fig. 1D and E), further demonstrating that Ad5Luc.FF/hCD40L does not require CAR for transduction of CD40-expressing cells. In contrast, pre-incubation with shCD40L decreased luciferase expression levels by 81% in 293/hCD40 cells, and by 78% in 293/cCD40 cells (Fig. 1D and E), but did not affect luciferase expression levels following Ad5Luc1 transduction in 293 cells (Fig. 1C). These results demonstrate that transduction by Ad5Luc.FF/hCD40L specifically requires cellular expression of CD40.

3.4. Targeted gene transfer to canine cells

To determine if CD40-targeted Ad5 also transduces canine DCs, as observed with DCs from other species, transduction experiments were conducted with canine DCs cultured from isolated PBMCs. Flow cytometry with anti-CD40 and -CD11c antibodies indicated CD40 expression on 43.5% of CD11c+ PBMCs (DCs), while only 1.7% of CD11c– cells were CD40+ (Fig. 2A). Based on CD40 expression, DCs were sorted into two groups: CD11c+/CD40– and CD11c+/CD40+. Cells from each group were incubated with either Ad5Luc1 or Ad5Luc.FF/hCD40L for analysis of transduction efficiency as measured by luciferase expression levels. As observed previously with human DCs [17], canine CD11c+/CD40+ DCs were refractory to transduction by untargeted Ad5, even at a very high vector concentration of 1000 vp/cell (Fig. 2B). In contrast, luciferase transgene expression was 15-fold higher in

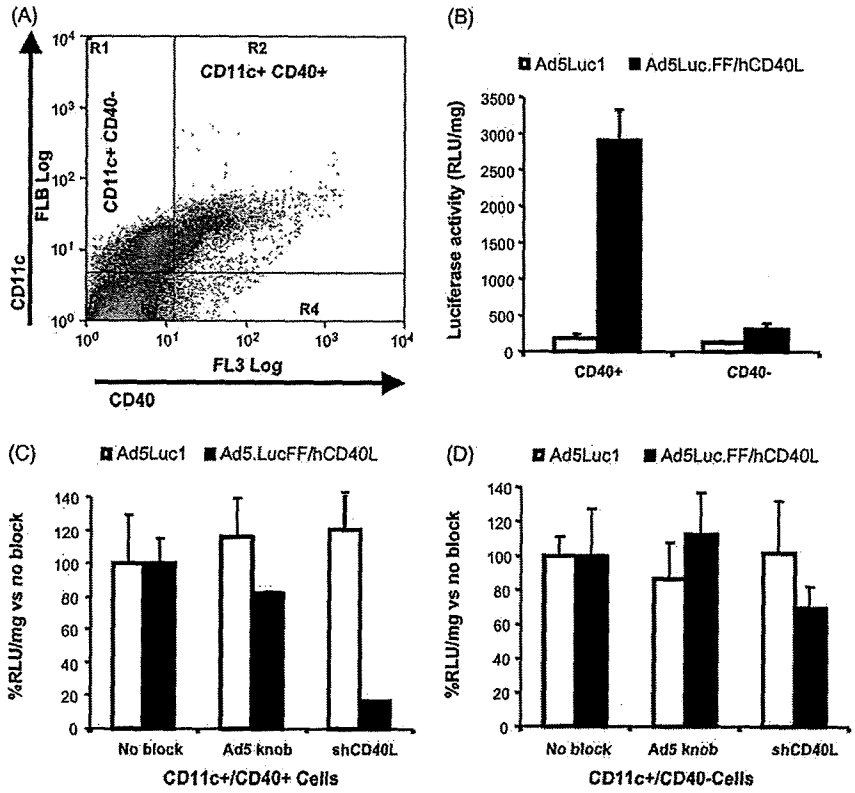

Fig. 2. Receptor specificity of cell transduction and efficiency of gene transfer mediated by CD40-targeted Ad5 in canine DCs. (A) Anti-CD40 antibodies detected expression of CD40 on 43.5% CD11c+ cells, and cells were sorted cells based on CD40 expression levels. (B) CD11c+/CD40+ and CD11c+/CD40– cells were transduced with untargeted Ad5Luc1 (white bars) or CD40-targeted Ad5Luc.FF/hCD40L (black bars) at an MOI of 1000 vp/cell to determine the receptor specificity of vector transduction. (C) CD11c+/CD40– and (D) CD11c+/CD40+ canine cells were transduced with untargeted Ad5Luc1 (white bars) or CD40-targeted Ad5Luc.FF/hCD40L (black bars) at an MOI of 1000 vp/cell in the presence of recombinant Ad5 fiber knob or soluble human CD40L to further confirm the receptor specificity of vector transduction. Luciferase activity detected in the presence of blocking agents is normalized against luciferase activity in absence of blocking agents. Mean ± *SD* are shown from three replicates performed simultaneously.

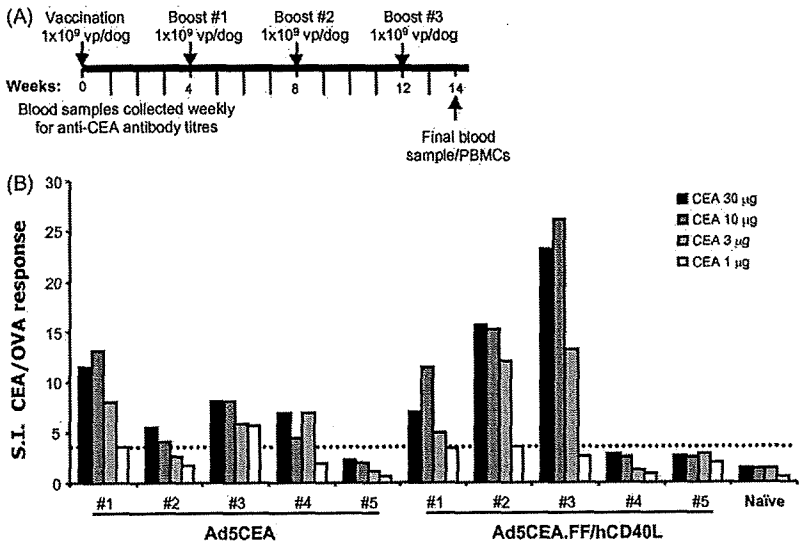

Fig. 3. Antigen-specific lymphocyte responses in healthy dogs vaccinated with CD40-targeted Ad5. (A) On day 0, five dogs were vaccinated i.d. with Ad5CEA (1×10^9 vp/dog) and five dogs were vaccinated with Ad5CEA.FF/hCD40L (1×10^9 vp/dog). At 4, 8 and 12 weeks post-vaccination, each dog received a booster injection (1×10^9 vp/dog) of the same vector. Blood was drawn at 14 weeks post-vaccination for lymphoproliferation assays. (B) Harvested PBMCs were stimulated for two days with recombinant human CEA at a range of concentrations (1–30 µg) or ovalbumin (25 µg) followed by an overnight pulse with tritiated thymidine. Cells were harvested and incorporated radioactivity was quantified. The S.I. was calculated as the mean cpm of the stimulated cells divided by the mean cpm of the ovalbumin-stimulated cells. A positive response was defined as a post-vaccination S.I. >3.0 (denoted by dotted line).

CD11c+/CD40+ DCs incubated with Ad5Luc.FF/hCD40L. Transgene expression was only slightly increased in CD11c+/CD40− DCs following incubation with Ad5Luc.FF/hCD40L, suggesting this vector specifically transduces cells via CD40. This minimal increase in Ad5Luc.FF/hCD40L-mediated gene transfer in CD11c+/CD40− DCs may be due to low-level expression of CD40 in this CD11c+ subset that could not be detected by flow analysis. Supporting this, luciferase expression was 84% lower in CD11c+/CD40+ cells pre-incubated with shCD40L and transduced with Ad5Luc.FF/hCD40L, but only 30% lower in CD11c+/CD40− cells pre-incubated with shCD40L (Fig. 2C and D). Furthermore, when transductions were performed with vectors encoding GFP, GFP expression was detected only in CD11c+/CD40+ cells incubated with the CD40-targeted vector. GFP expression was not detected in CD11c+/CD40− cells incubated with CD40-targeted vector or in either DC subset incubated with untargeted vector (Supplementary Fig. 1). These results again confirm the specificity of CD40-mediated transduction by this CD40-targeted Ad5 vector. Thus, the efficient and specific delivery of transgenes to canine DCs by Ad5Luc.FF/hCD40L *in vitro* validates the examination of this vector for *in vivo* delivery of transgenes to CD40-expressing cells, particularly DCs.

3.5. Antigen-specific immune responses following vaccination in healthy dogs

The ultimate goal is the development of a vaccine that can deliver tumor-specific transgenes to DCs *in vivo* in order to generate a TAA-specific immune response. Therefore, it was critical to investigate the capacity of untargeted versus CD40-targeted Ad5 vectors to induce TAA-specific immune responses. We have previously demonstrated an enhanced immune response in mice following injection of CD40-targeted Ad5 by various routes [25]. To determine if similar immune responses are detected in dogs, we performed a pilot experiment with healthy dogs injected with Ad5 vectors engineered to express human carcinoembryonic antigen (CEA) as a model tumor antigen (Ad5CEA and Ad5CEA.FF/hCD40L). CEA orthologues have been identified in dogs; however xenoantigens are more likely to overcome immunotolerance and induce a more robust antigen-specific immune response [42–45]. Five dogs received i.d. injections of Ad5CEA (1×10^9 vp/injection) and five dogs received injections of Ad5CEA.FF/hCD40L (1×10^9 vp/injection) according to the schedule outlined in Fig. 3A. One dog served as a negative control, receiving no injections. At week 14, PBMCs were harvested and lymphocyte proliferation was quantified as a measure of TAA-specific T cell activation. An S.I. of greater than 3.0 was considered positive. A positive lymphoproliferative response was observed in three of five dogs immunized with Ad5CEA.FF/hCD40L and in four of five dogs immunized with Ad5CEA, although the average S.I. tended to be greater in responding animals immunized with Ad5CEA.FF/hCD40L (Fig. 3B). These results suggest that while vaccination with either untargeted or CD40-targeted Ad5 induces an antigen-specific T cell response, this response may be magnified in individuals responding to the CD40-targeted vector.

To analyze antigen-specific humoral immune responses, CEA-specific IgG serum concentrations were quantified. A strong anti-CEA humoral immune response was induced in both groups of dogs by 14 days post-immunization, though the antibody titer of dogs immunized with untargeted Ad5CEA was significantly higher as measured on days 21, 35 and 42 (Fig. 4A). We further examined the isotype of the antibody response on day 35, the day with the most significant difference in antibody responses between the groups. The concentration of IgG1 was significantly lower in dogs immunized with Ad5CEA.FF/hCD40L (Fig. 4B and C), resulting in a higher ratio of IgG2 to IgG1 (Fig. 4D).

4. Discussion

DC-based vaccination can overcome tumor-associated suppression of immune responses, although the full potential of this strategy has yet to be realized in the context of a reliable cancer therapy [4–8]. In order to overcome the potential limitations associated with autologous DCs transduced and matured *ex vivo*, our lab has investigated methods to directly transduce and activate DCs *in vivo* in a an animal model highly likely to provide clinically relevant information.

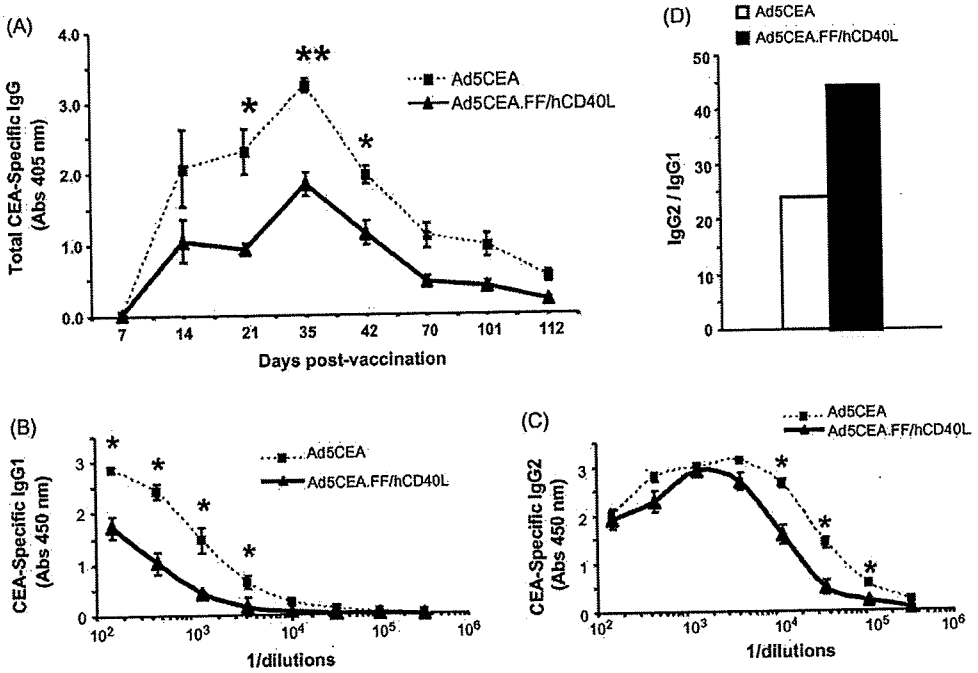

Fig. 4. Antigen-specific humoral responses in healthy dogs vaccinated with CD40-targeted Ad5. (A) Serum was drawn weekly from each dog following vaccination with Ad5CEA (squares) or Ad5CEA.FF/hCD40L (triangles). ELISAs were performed to detect human CEA-specific canine IgGs. Serum from each time point was incubated with recombinant human CEA, and detected with anti-dog IgG secondary antibody to determine total IgG concentrations. (B) IgG1 and (C) IgG2 isotypes were detected with goat anti-dog IgG1 and sheep anti-dog IgG2 antibodies, respectively. (A, B and C) Absorbance was read at 450 nm. Statistical analysis for was performed by using two-tailed Student's *t*-test and values are presented as mean ± SE. $^{*}p < 0.05$; $^{**}p < 0.0001$. (D) Average ratio of IgG2:IgG1 following vaccination with Ad5CEA (white) or Ad5CEA.FF/hCD40L (black).

Several strategies to accomplish *in vivo* delivery of immunotherapeutic antigens to DCs have now been reported, including the use of free antigen, protein fusions and viral gene therapy [46–51]. However, complete success depends on overcoming biological delivery challenges. In this regard, Arthur et al. previously found that Ad5 vectors are superior to other non-viral methods for delivering antigens to DCs *in vitro* [10], and other groups have since demonstrated highly efficient Ad5-mediated gene transfer to DCs *ex vivo*, using high concentrations of Ad5 [52,53]. Additionally, Ad5 capsid protein is a potent adjuvant that enhances CTL response [54]. Therefore, TAA transfer by Ad5 vectors is likely to enhance production of tumor cell-specific CTL [55]. Thus, an Ad5 vector re-targeted to bind a specific protein expressed on the surface of DCs seems likely to provide an enhanced *in vivo* immunotherapeutic strategy.

In addition to targeting DCs, proper activation and maturation of DCs is crucial for stimulating an antigen-specific immune response. It is now obvious that the collective term "DC" actually refers to a heterogeneous population of cells, derived from different lineages, in different maturation states, and likely displaying distinct functional features [8]. In general, antigen presentation by mature DCs leads to an antigen-specific immune response, while antigen presentation by immature DCs has been implicated in the induction of immune tolerance through activation of regulatory T cells [56]. CD40 is an attractive candidate for targeting DCs as it is expressed on the cell surface of DCs, and, while it is also expressed on endothelial cells and other immune cells, CD40 expression is far less ubiquitous than CAR expression. Additionally, localized dermal injection of CD40-targeted virus delivers virus to a location that is rich in CD40-positive DCs and lacks substantial numbers of other CD40-expressing cells, such as B cells. Binding of CD40L to CD40 induces DC maturation, enabling these cells to migrate to draining lymph nodes and activate antigen-specific T cells. This complete activation of DCs is critical for tumor rejection *in vivo* [57].

Results from the analysis of our *in vitro* gene transfer in model cell lines and canine DCs demonstrates CD40-targeting dramatically enhances Ad5-mediated transgene expression in cells expressing CD40, and in DCs in particular. Furthermore, CD40-targeted Ad5 requires cell expression of CD40 for transduction, and is incapable of transducing cells through CAR. This specificity will likely allow *in vivo* transduction of DCs with a much lower vector dose than is required for untargeted Ad5 transduction. Studies are currently underway to confirm the *in vivo* cell specificity of CD40-targeting.

In order to obtain clinically relevant information regarding the immune response generated *in vivo* following vaccination with CD40-targeted Ad5, we immunized healthy dogs with CD40-targeted or untargeted Ad5 encoding human CEA as a model tumor antigen. A key issue in the successful development of effective cancer immunotherapies is the design of vaccines that can overcome immune tolerance and induce a T cell response to autologous TAA, which are also expressed by normal cells. In this regard, experiments in mouse models suggested that vaccination with xenogeneic TAAs (xenoantigens) encoding slight differences in sequence overcome immune tolerance by improving MHC I and II epitope presentation, evoking tumor immunity [42–45]. Thus, using Ad5 vectors encoding human CEA allowed us to more thoroughly investigate the potential of eliciting TAA-specific immune responses in dogs via a CD40-targeted Ad5 vector.

Antigen-specific T cell responses were generated in dogs receiving either the CD40-targeted vector or the untargeted vector. Interestingly, the extent of lymphoproliferation appeared to be enhanced in responders immunized with CD40-targeted Ad5 as compared to untargeted Ad5, though these responses will need to be investigated with a larger number of dogs in order to thoroughly evaluate statistical significance. Further, as observed with previous studies in mice [25], an antigen-specific humoral response was also observed following vaccination with either CD40-targeted

or untargeted vectors in all dogs. However, a clear difference in the quality of the response was detected in the ratio of IgG1 to IgG2 isotypes generated by the two vectors. Though the relationship between Th type responses and IgG subclass has not been completely characterized in dogs [58], previous reports suggest that increased IgG2 production correlates with a Th1 type immune response that is characterized by a cytokine profile similar to that in humans [59–62]. Also similar to human patients, Th1 inducing cells, as determined by cytokine production, are diminished in dogs with metastatic cancers [63]. Suppression of DC-activated Th1 immunity has been implicated in the progression of cancers such as melanoma, thus an enhanced antigen-specific Th1 cellular immune response is likely to result in a more effective anti-tumor response. Future studies measuring cytokine release by T cells will be required for complete evaluation of the immune response generated, however.

In summary, these results from a pilot vaccination study in dogs confirm in a clinically relevant animal model that re-targeting Ad5 to bind CD40 circumvents the requirement for CAR expression, allowing efficient transgene expression in DCs *in vitro*, and subsequent antigen-specific immune responses *in vivo*. CD40-targeted Ad5 may in turn provide more effective cancer therapies. Most importantly, immune responses in these dogs are comparable to expected responses in humans, and establish that dogs provide a reliable intermediate model system for investigating potential immunotherapies for cancers such as osteosarcoma, lymphoma, breast cancer and melanoma. Thus, these experiments have provided the critical groundwork necessary to allow further evaluation of targeted immunotherapies in canine cancer patients in order to provide information for development of successful translational therapies.

Acknowledgements

The authors thank A. Church Bird for valuable consultations on FACs and flow cytometry, Dr. Sandra Ewald for critical advice for optimizing DC culture conditions, and Dr. Maaike Everts for critical reading of the manuscript. This work was supported by: 1R01 CA113454 to BFS, NIAMS P30-AR050948 to LT and NIH training grants T32 CA075930-09 and T32 AR053458-01 to ET.

Appendix A. Supplementary data

Supplementary data associated with this article can be found, in the online version, at doi:10.1016/j.vaccine.2009.09.055.

References

[1] Chen L. Immunological ignorance of silent antigens as an explanation of tumor evasion. Immunol Today 1998;19(1):27–30.
[2] Geijtenbeek TB, van Vliet SJ, Engering A, t Hart BA, van Kooyk Y. Self- and nonself-recognition by C-type lectins on dendritic cells. Annu Rev Immunol 2004;22:33–54.
[3] O'Hagan DT, Valiante NM. Recent advances in the discovery and delivery of vaccine adjuvants. Nat Rev Drug Discov 2003;2(9):727–35.
[4] Mosca PJ, Lyerly HK, Clay TM, Morse MA, Lyerly HK. Dendritic cell vaccines. Front Biosci 2007;12:4050–60.
[5] Cerundolo V, Hermans IF, Salio M. Dendritic cells: a journey from laboratory to clinic. Nat Immunol 2004;5(1):7–10.
[6] den Brok MH, Nierkens S, Figdor CG, Ruers TJ, Adema GJ. Dendritic cells: tools and targets for antitumor vaccination. Expert Rev Vaccines 2005;4(5):699–710.
[7] Tuyaerts S, Aerts JL, Corthals J, Neyns B, Heirman C, Breckpot K, et al. Current approaches in dendritic cell generation and future implications for cancer immunotherapy. Cancer Immunol Immunother 2007;56(10):1513–37.
[8] Lesterhuis WJ, Aarntzen EH, De Vries IJ, Schuurhuis DH, Figdor CG, Adema GJ, et al. Dendritic cell vaccines in melanoma: from promise to proof? Crit Rev Oncol Hematol 2008;66(2):118–34.
[9] Proudfoot O, Apostolopoulos V, Pietersz GA. Receptor-mediated delivery of antigens to dendritic cells: anticancer applications. Mol Pharm 2007;4(1):58–72.
[10] Arthur JF, Butterfield LH, Roth MD, Bui LA, Kiertscher SM, Lau R, et al. A comparison of gene transfer methods in human dendritic cells. Cancer Gene Ther 1997;4(1):17–25.
[11] Lotem M, Zhao Y, Riley J, Hwu P, Morgan RA, Rosenberg SA, et al. Presentation of tumor antigens by dendritic cells genetically modified with viral and nonviral vectors. J Immunother 2006;29(6):616–27.
[12] van Leeuwen EB, Cloosen S, Senden-Gijsbers BL, Germeraad WT, Bos GM. Transduction with a fiber-modified adenoviral vector is superior to non-viral nucleofection for expressing tumor-associated Ag mucin-1 in human DC. Cytotherapy 2006;8(1):36–46.
[13] Zhong L, Granelli-Piperno A, Choi Y, Steinman RM. Recombinant adenovirus is an efficient and non-perturbing genetic vector for human dendritic cells. Eur J Immunol 1999;29(3):964–72.
[14] Zhang L, Tang Y, Akbulut H, Zelterman D, Linton PJ, Deisseroth AB. An adenoviral vector cancer vaccine that delivers a tumor-associated antigen/CD40-ligand fusion protein to dendritic cells. Proc Natl Acad Sci USA 2003;100(25):15101–6.
[15] Cho HI, Kim HJ, Oh ST, Kim TG. In vitro induction of carcinoembryonic antigen (CEA)-specific cytotoxic T lymphocytes by dendritic cells transduced with recombinant adenoviruses. Vaccine 2003;22(2):224–36.
[16] Noureddini SC, Curiel DT. Genetic targeting strategies for adenovirus. Mol Pharm 2005;2(5):341–7.
[17] Tillman BW, de Gruijl TD, Luykx-de Bakker SA, Scheper RJ, Pinedo HM, Curiel TJ, et al. Maturation of dendritic cells accompanies high-efficiency gene transfer by a CD40-targeted adenoviral vector. J Immunol 1999;162(11):6378–83.
[18] Pereboev AV, Nagle JM, Shakhmatov MA, Triozzi PL, Matthews QL, Kawakami Y, et al. Enhanced gene transfer to mouse dendritic cells using adenoviral vectors coated with a novel adapter molecule. Mol Ther 2004;9(5):712–20.
[19] Izumi M, Kawakami Y, Glasgow JN, Belousova N, Everts M, Kim-Park S, et al. In vivo analysis of a genetically modified adenoviral vector targeted to human CD40 using a novel transient transgenic model. J Gene Med 2005;7(12):1517–25.
[20] Korokhov N, Noureddini SC, Curiel DT, Santegoets SJ, Scheper RJ, de Gruijl TD. A single-component CD40-targeted adenovirus vector displays highly efficient transduction and activation of dendritic cells in a human skin substrate system. Mol Pharm 2005;2(3):218–23.
[21] Belousova N, Korokhov N, Krendelshchikova V, Simonenko V, Mikheeva G, Triozzi PL, et al. Genetically targeted adenovirus vector directed to CD40-expressing cells. J Virol 2003;77(21):11367–77.
[22] Clement A, Pereboev A, Curiel DT, Dong SS, Hutchings A, Thomas JM. Converting nonhuman primate dendritic cells into potent antigen-specific cellular immunosuppressants by genetic modification. Immunol Res 2002;26(1–3):297–302.
[23] de Gruijl TD, Luykx-de Bakker SA, Tillman BW, van den Eertwegh AJ, Buter J, Lougheed SM, et al. Prolonged maturation and enhanced transduction of dendritic cells migrated from human skin explants after in situ delivery of CD40-targeted adenoviral vectors. J Immunol 2002;169(9):5322–31.
[24] Pereboev AV, Asiedu CK, Kawakami Y, Dong SS, Blackwell JL, Kashentseva EA, et al. Coxsackievirus-adenovirus receptor genetically fused to anti-human CD40 scFv enhances adenoviral transduction of dendritic cells. Gene Ther 2002;9(17):1189–93.
[25] Huang D, Pereboev AV, Korokhov N, He R, Larocque L, Gravel C, et al. Significant alterations of biodistribution and immune responses in Balb/c mice administered with adenovirus targeted to CD40(+) cells. Gene Ther 2008;15(4):298–308.
[26] Paoloni M, Khanna C. Translation of new cancer treatments from pet dogs to humans. Nat Rev Cancer 2008;8(2):147–56.
[27] Khanna C, Lindblad-Toh K, Vail D, London C, Bergman P, Barber L, et al. The dog as a cancer model. Nat Biotechnol 2006;24(9):1065–6.
[28] Porrello A, Cardelli P, Spugnini EP. Oncology of companion animals as a model for humans. An overview of tumor histotypes. J Exp Clin Cancer Res 2006;25(1):97–105.
[29] Waters DJ, Wildasin K. Cancer clues from pet dogs. Sci Am 2006;295(6):94–101.
[30] Smith BF, Baker HJ, Curiel DT, Jiang W, Conry RM. Humoral and cellular immune responses of dogs immunized with a nucleic acid vaccine encoding human carcinoembryonic antigen. Gene Ther 1998;5(7):865–8.
[31] Casal M, Haskins M. Large animal models and gene therapy. Eur J Hum Genet 2006;14(3):266–72.
[32] Seki T, Dmitriev I, Kashentseva E, Takayama K, Rots M, Suzuki K, et al. Artificial extension of the adenovirus fiber shaft inhibits infectivity in coxsackievirus and adenovirus receptor-positive cell lines. J Virol 2002;76(3):1100–8.
[33] Krasnykh V, Belousova N, Korokhov N, Mikheeva G, Curiel DT. Genetic targeting of an adenovirus vector via replacement of the fiber protein with the phage T4 fibritin. J Virol 2001;75(9):4176–83.
[34] Graham FL, Prevec L. Methods for construction of adenovirus vectors. Mol Biotechnol 1995;3(3):207–20.
[35] Oster W, Lindemann A, Mertelsmann R, Herrmann F. Regulation of gene expression of M-, G-, GM-, and multi-CSF in normal and malignant hematopoietic cells. Blood Cells 1988;14(2–3):443–62.
[36] Lu L, Srour EF, Warren DJ, Walker D, Graham CD, Walker EB, et al. Enhancement of release of granulocyte- and granulocyte-macrophage colony-stimulating factors from phytohemagglutinin-stimulated sorted subsets of human T lymphocytes by recombinant human tumor necrosis factor-alpha. Synergism with recombinant human IFN-gamma. J Immunol 1988;141(1):201–7.

[37] Krasnykh VN, Mikheeva GV, Douglas JT, Curiel DT. Generation of recombinant adenovirus vectors with modified fibers for altering viral tropism. J Virol 1996;70(10):6839–46.
[38] Perreau M, Mennechet F, Serratrice N, Glasgow JN, Curiel DT, Wodrich H, et al. Contrasting effects of human, canine, and hybrid adenovirus vectors on the phenotypical and functional maturation of human dendritic cells: implications for clinical efficacy. J Virol 2007;81(7):3272–84.
[39] Korokhov N, Mikheeva G, Krendelshchikov A, Belousova N, Simonenko V, Krendelshchikova V, et al. Targeting of adenovirus via genetic modification of the viral capsid combined with a protein bridge. J Virol 2003;77(24):12931–40.
[40] Bajorath J, Chalupny NJ, Marken JS, Siadak AW, Skonier J, Gordon M, et al. Identification of residues on CD40 and its ligand which are critical for the receptor-ligand interaction. Biochemistry 1995;34(6):1833–44.
[41] Bajorath J. Detailed comparison of two molecular models of the human CD40 ligand with an X-ray structure and critical assessment of model-based mutagenesis and residue mapping studies. J Biol Chem 1998;273(38):24603–9.
[42] Weber LW, Bowne WB, Wolchok JD, Srinivasan R, Qin J, Moroi Y, et al. Tumor immunity and autoimmunity induced by immunization with homologous DNA. J Clin Invest 1998;102(6):1258–64.
[43] Gold JS, Ferrone CR, Guevara-Patino JA, Hawkins WG, Dyall R, Engelhorn ME, et al. A single heteroclitic epitope determines cancer immunity after xenogeneic DNA immunization against a tumor differentiation antigen. J Immunol 2003;170(10):5188–94.
[44] Naftzger C, Takechi Y, Kohda H, Hara I, Vijayasaradhi S, Houghton AN. Immune response to a differentiation antigen induced by altered antigen: a study of tumor rejection and autoimmunity. Proc Natl Acad Sci USA 1996;93(25):14809–14.
[45] Hawkins WG, Gold JS, Dyall R, Wolchok JD, Hoos A, Bowne WB, et al. Immunization with DNA coding for gp100 results in CD4 T-cell independent antitumor immunity. Surgery 2000;128(2):273–80.
[46] Mahnke K, Qian Y, Fondel S, Brueck J, Becker C, Enk AH. Targeting of antigens to activated dendritic cells in vivo cures metastatic melanoma in mice. Cancer Res 2005;65(15):7007–12.
[47] Hauser H, Shen L, Gu QL, Krueger S, Chen SY. Secretory heat-shock protein as a dendritic cell-targeting molecule: a new strategy to enhance the potency of genetic vaccines. Gene Ther 2004;11(11):924–32.
[48] Bonifaz LC, Bonnyay DP, Charalambous A, Darguste DI, Fujii S, Soares H, et al. In vivo targeting of antigens to maturing dendritic cells via the DEC-205 receptor improves T cell vaccination. J Exp Med 2004;199(6):815–24.
[49] Yang L, Yang H, Rideout K, Cho T, Joo KI, Ziegler L, et al. Engineered lentivector targeting of dendritic cells for in vivo immunization. Nat Biotechnol 2008;26(3):326–34.
[50] Kretz-Rommel A, Qin F, Dakappagari N, Torensma R, Faas S, Wu D, et al. In vivo targeting of antigens to human dendritic cells through DC-SIGN elicits stimulatory immune responses and inhibits tumor growth in grafted mouse models. J Immunother 2007;30(7):715–26.
[51] Pereira CF, Torensma R, Hebeda K, Kretz-Rommel A, Faas SJ, Figdor CG, et al. In vivo targeting of DC-SIGN-positive antigen-presenting cells in a nonhuman primate model. J Immunother 2007;30(7):705–14.
[52] Mossoba ME, Medin JA. Cancer immunotherapy using virally transduced dendritic cells: animal studies and human clinical trials. Expert Rev Vaccines 2006;5(5):717–32.
[53] Basak SK, Kiertscher SM, Harui A, Roth MD. Modifying adenoviral vectors for use as gene-based cancer vaccines. Viral Immunol 2004;17(2):182–96.
[54] Molinier-Frenkel V, Lengagne R, Gaden F, Hong SS, Choppin J, Gahery-Segard H, et al. Adenovirus hexon protein is a potent adjuvant for activation of a cellular immune response. J Virol 2002;76(1):127–35.
[55] Banchereau J. The long arm of the immune system. Sci Am 2002;287(5):52–9.
[56] Finkelman FD, Lees A, Birnbaum R, Gause WC, Morris SC. Dendritic cells can present antigen in vivo in a tolerogenic or immunogenic fashion. J Immunol 1996;157(4):1406–14.
[57] Mackey MF, Gunn JR, Maliszewsky C, Kikutani H, Noelle RJ, Barth Jr RJ. Dendritic cells require maturation via CD40 to generate protective antitumor immunity. J Immunol 1998;161(5):2094–8.
[58] Day MJ. Immunoglobulin. G subclass distribution in canine leishmaniosis: a review and analysis of pitfalls in interpretation. Vet Parasitol 2007;147(1–2):2–8.
[59] Carvalho LH, Sano G, Hafalla JC, Morrot A, Curotto de Lafaille MA, Zavala F. IL-4-secreting CD4+ T cells are crucial to the development of CD8+ T-cell responses against malaria liver stages. Nat Med 2002;8(2):166–70.
[60] Boag PR, Parsons JC, Presidente PJ, Spithill TW, Sexton JL. Characterisation of humoral immune responses in dogs vaccinated with irradiated *Ancylostoma caninum*. Vet Immunol Immunopathol 2003;92(1–2):87–94.
[61] Fujiwara RT, Loukas A, Mendez S, Williamson AL, Bueno LL, Wang Y, et al. Vaccination with irradiated *Ancylostoma caninum* third stage larvae induces a Th2 protective response in dogs. Vaccine 2006;24(4):501–9.
[62] Breathnach RM, Fanning S, Mulcahy G, Bassett HF, Jones BR, Daly P. Evaluation of Th1-like, Th2-like and immunomodulatory cytokine mRNA expression in the skin of dogs with immunomodulatory-responsive lymphocytic–plasmacytic pododermatitis. Vet Dermatol 2006;17(5):313–21.
[63] Horiuchi Y, Hanazawa A, Nakajima Y, Nariai Y, Asanuma H, Kuwabara M, et al. T-helper (Th)1/Th2 imbalance in the peripheral blood of dogs with malignant tumor. Microbiol Immunol 2007;51(11):1135–8.

Enhanced Antitumor Effects of an Engineered Measles Virus Edmonston Strain Expressing the Wild-type *N*, *P*, *L* Genes on Human Renal Cell Carcinoma

Xin Meng[1,2], Takafumi Nakamura[3,4], Toshihiko Okazaki[1], Hiroyuki Inoue[1], Atsushi Takahashi[1], Shohei Miyamoto[1], Gaku Sakaguchi[5], Masatoshi Eto[5], Seiji Naito[5], Makoto Takeda[6], Yusuke Yanagi[6] and Kenzaburo Tani[1]

[1]Department of Molecular Genetics, Medical Institute of Bioregulation, Kyushu University, Fukuoka, Japan; [2]Department of Biochemistry and Molecular Biology, China Medical University, Shenyang, China; [3]Core Facility for Therapeutic Vectors, The Institute of Medical Science, The University of Tokyo, Tokyo, Japan; [4]RNA and Biofunctions, PRESTO, Japan Science and Technology Agency, Saitama, Japan; [5]Department of Urology, Graduate School of Medical Sciences, Kyushu University, Fukuoka, Japan; [6]Department of Virology, Faculty of Medicine, Kyushu University, Fukuoka, Japan

Measles virus Edmonston strain (MV-Edm) is thought to have remarkable oncolytic activity that selectively destroys human tumor cells. The P/V/C protein of wild-type MV was shown to resist the antiviral effects of interferon (IFN)-α. Here, we engineered new MVs by arming MV-Edm tag strain (a V-defective vaccine-lineage strain, MV-Etag) with the *P* or *N*, *P*, and *L* genes of wild-type MV (MV-P and MV-NPL, respectively). The oncolytic activities of the MVs were determined in human renal cell carcinoma (RCC) cell lines and primary human RCC cells by the MTT assay. The antitumor efficacy of the MVs was evaluated in A-498 xenografts in nude mice. IFN-α effectively inhibited the replication of MV-Etag and MV-P, but not MV-NPL. MV-NPL more efficiently induced cytopathic effects (CPEs) in OS-RC-2 cells, even in the presence of human IFN-α. MV-NPL replicated more rapidly than MV-P and MV-Etag in A-498 cells. Apoptosis was induced earlier in A-498 cells by MV-NPL than MV-Etag and MV-P. MV-NPL showed more significant antitumoral effects and had prolonged replication compared to MV-Etag and MV-P. In this study, we demonstrated that the newly engineered MV-NPL has more effective oncolytic activity and may help establish an innovative cancer therapy.

Received 31 August 2009; accepted 2 December 2009; advance online publication 5 January 2010. doi:10.1038/mt.2009.296

INTRODUCTION

Oncovirotherapy, which uses replication-competent viruses as a cancer therapy, is attracting much interest.[1–4] Recently, several reports confirmed that these live-attenuated viruses can induce rapid and lytic infections in tumor cells.[5–10] Furthermore, some viruses are being used as cancer therapies in current clinical trials.[4,11,12] Measles virus Edmonston strain (MV-Edm) has potent antineoplastic activity against various human cancers, including lymphoma, ovarian cancer, mesothelioma, breast cancer, and hepatocellular carcinoma.[11,13–16] It selectively induces potent cytopathic effects (CPEs), notably intercellular fusion in cancer cells, but causes minimal damage in normal cells.[9,17] In addition, the MV genome is very stable and the vaccine strains have never reverted to pathogenic forms, making MV highly suitable for further development as an oncolytic agent.

Measles virus is a negative-strand RNA virus of the Morbillivirus genus in the *Paramyxoviridae* family. A polymerase (L) and its cofactor (P) associate with the viral RNA and N protein to form a ribonucleoprotein. This complex is surrounded by the M protein. The *P* gene encodes the P protein and two nonstructural accessory proteins, C and V.[18] The two MV envelope glycoproteins H and F work in concert to induce virus–cell membrane fusion. CD46 and CD150 were identified as two MV receptors. CD150 expression is confined to immune cells, whereas CD46 is expressed ubiquitously in nucleated cells.[19–21] CD46 is abundantly expressed in cancer cells,[22,23] but minimally expressed in normal cells such as fibroblasts and peripheral blood lymphocytes,[9,17] making cancer cells a suitable target for MV oncolytic therapy.

Type I interferon (IFN-α/β) is a powerful innate antiviral defense. MV vaccine strains can induce significantly higher levels of type I IFN than wild-type MV.[24] To combat the cellular innate immune response, many viruses encode antagonistic molecules that block some steps of the type I IFN antiviral response.[25] The P proteins of wild-type MV have been shown to resist type I IFN. Furthermore, an engineered MV-Edm tag strain (MV-P), whose *P* gene was replaced with the comparable wild-type gene, induces significantly less IFN-α in tumor cells and has enhanced oncolytic potency against human multiple myeloma compared to the parental virus.[13] The major function of the N protein is to surround the genomic RNA, encapsidate the viral genome, and support

Correspondence: Kenzaburo Tani, Department of Molecular Genetics Medical Institute of Bioregulation, Kyushu University, Fukuoka 812-8582, Japan. E-mail: taniken@bioreg.kyushu-u.ac.jp